Propagation of moments in Hawkes networks

Matthieu Gilson[1] and Jean-Pascal Pfister[2,3]

[1]Universitat Pompeu Fabra, Barcelona, Spain
[2]Institute of Neuroinformatics and Neuroscience Center Zurich, University of Zurich/ETH Zurich, Zurich, Switzerland
[3]Department of Physiology, University of Bern, Bern, Switzerland

October 24, 2018

Abstract

The present paper provides a mathematical description of high-order moments of spiking activity in a recurrently-connected network of Hawkes processes. It extends previous studies that have explored the case of a (linear) Hawkes network driven by deterministic rate functions to the case of a stimulation by external inputs (rate functions or spike trains) with arbitrary correlation structure. Our approach describes the spatio-temporal filtering induced by the afferent and recurrent connectivities using operators of the input moments. This algebraic viewpoint provides intuition about how the network ingredients shape the input-output mapping for moments, as well as cumulants.

1 Introduction

Immense efforts in neuroscience have been invested in measuring neuronal activity as well as the detailed connectivity between neurons. Such studies have been too often conducted separately, despite the fact that neuronal activity and synaptic connectivity are deeply intertwined. Indeed, the synaptic connectome determines the neuronal activity, while the latter reshapes the connectome through activity-dependent plasticity. To better understand the intricate link between activity and connectivity at the neuronal level, it is important to build tractable network models that relate one to the other.

In this paper we analytically compute the statistics of neuronal activity —described via moments and cumulants— from the connectivity. In particular, we investigate how the spiking statistics propagates from an input population of neurons to an output population of recurrently-connected neurons as a function of the synaptic kernels, see Fig. 1A.

In order to remain tractable, the neuronal activity is modeled using a Hawkes process (Hawkes 1971a; Hawkes 1971b), also known as (linear) Poisson neurons (Kempter, Gerstner, and Van Hemmen 1999) whose firing activity depends on upstream neurons as represented in Fig. 1B and C. Here we refer to the multivariate Hawkes process as Hawkes network. Hawkes' model has attracted much attention in various disciplines such as neuroscience (Gilson, Burkitt, and van Hemmen 2010; Mei and Eisner 2017), artificial intelligence (Etesami, Kiyavash, Zhang, and Singhal 2016), seismology (Le 2018; Lima and Choi 2018), epidemiology (Saichev, Maillart, and Sornette 2013) and finance (Errais, Giesecke, and Goldberg 2010; Bacry, Mastromatteo, and Muzy 2015). Due to the event-like nature of its activity, intrinsic correlations arise and reverberate as echoes induced by the recurrent connectivity. The present study builds upon Hawkes' results that describe second-order correlations for mutually exciting point processes (Hawkes 1971a; Hawkes 1971b) and extends them to higher orders. In particular, we show how moments of arbitrary order propagate from one layer to the next.

The vast majority of studies focuses on the first and second orders of spiking statistics (Hawkes 1971a; Hawkes 1971b; Gilson, Burkitt, and van Hemmen 2010; Brémaud, Massoulié, and Ridolfi 2005; Tannenbaum and Burak 2017). Up to our knowledge, only two recent studies have investigated higher-order cumulants (Jovanović, Hertz, and Rotter 2015; Ocker, Josić, Shea-Brown, and Buice 2017). In the earliest (Jovanović, Hertz, and Rotter 2015), the authors derived a recursive algorithm based on the theory of branching Hawkes processes to calculate the cumulants for the spiking activity. The second study (Ocker, Josić, Shea-Brown, and Buice 2017) relies on path-integral representation to explore the cumulants, which are closely related to moments, for Hawkes process with possible non-linearities. If the path-integral representation derived from field theory is adequate to tackle non-linearities, it provide limited intuition on the geometrical aspect for the transmission of spiking density across layers. A common limitation of both studies is that they provide little intuition about how the moments propagate in neuronal networks, which we aim to address here. Moreover, the case of neurons stimulated by inputs with correlated activity has not been explored yet for larger-than-second orders.

A motivation for investigating higher-than-second orders of correlations in Hawkes networks comes from the study of spike-timing dependent plasticity (STDP). The established formula (Hawkes 1971a) is sufficient to analyze in recurrently-connected networks the effect of the so-called pairwise STDP: As the synaptic weights between neurons are modified depending on the time difference between input and output spikes, the overall effect can be captured by the spiking covariances (Gilson, Burkitt, Grayden, Thomas, and van Hemmen 2009a; Gilson, Burkitt, Grayden, Thomas, and van Hemmen 2009b; Pfister and Tass 2010). However, the more elaborate model of triplet STDP (Pfister and Gerstner 2006; Gjorgjieva, Clopath, Audet, and Pfister 2011) requires the knowledge about the third order of the spike statistics, involving input-output-output spikes. To gain intuition, a key is understanding how the synaptic connectivity shapes the input correlation structure in a network as illustrated in Fig. 1A.

Another motivation is that, although pairwise correlations have been argued to be sufficient to represent experimental data (Barreiro, Gjorgjieva, Rieke, and Shea-Brown 2014), this view has been recently challenged and mechanisms related to higher-order correlations have been found to improve descriptive statistical models (Shimazaki, Sadeghi, Ishikawa, Ikegaya, and Toyoizumi 2015). In dynamic neuron models, even though population mean-field dynamics can be captured by non-spiking models (Helias, Tetzlaff, and Diesmann 2013; Grytskyy, Tetzlaff, Diesmann, and Helias 2013), networks with realistic sizes exhibit finite-size effects in their pairwise correlations (van Albada, Helias, and Diesmann 2015). This calls for analytical techniques to evaluate those at arbitrary orders, as was done recently for binary neurons (Dahmen, Bos, and Helias 2016).

This led us to investigate a general solution for the spatio-temporal correlation structure via moments of arbitrary orders in Hawkes processes as a function of the moments in the input population. Our results are structured around three theorems. The first one describes how moments (of arbitrary orders) propagate in feedforward networks, thereby generalizing the results by (Kempter, Gerstner, and Van Hemmen 1999). The second theorem describes the effect of recurrent connectivitywithin the output population, extending (Gilson, Burkitt, Grayden, Thomas, and van Hemmen 2009b; Pfister and Tass 2010). The last theorem translates the mappings for moments into mappings for cumulants, in line with a recent line of work (Jovanović, Hertz, and Rotter 2015; Ocker, Josić, Shea-Brown, and Buice 2017).

2 Results

Let us consider an input population of m neurons whose spiking activity (superposition of Dirac deltas at spike times) is denoted by the vector of functions $x(t) = (x_1(t), \cdots, x_m(t))$. This input population together with some stochastic input rates $\lambda(t) = (\lambda_1(t), \cdots, \lambda_n(t))$ feed

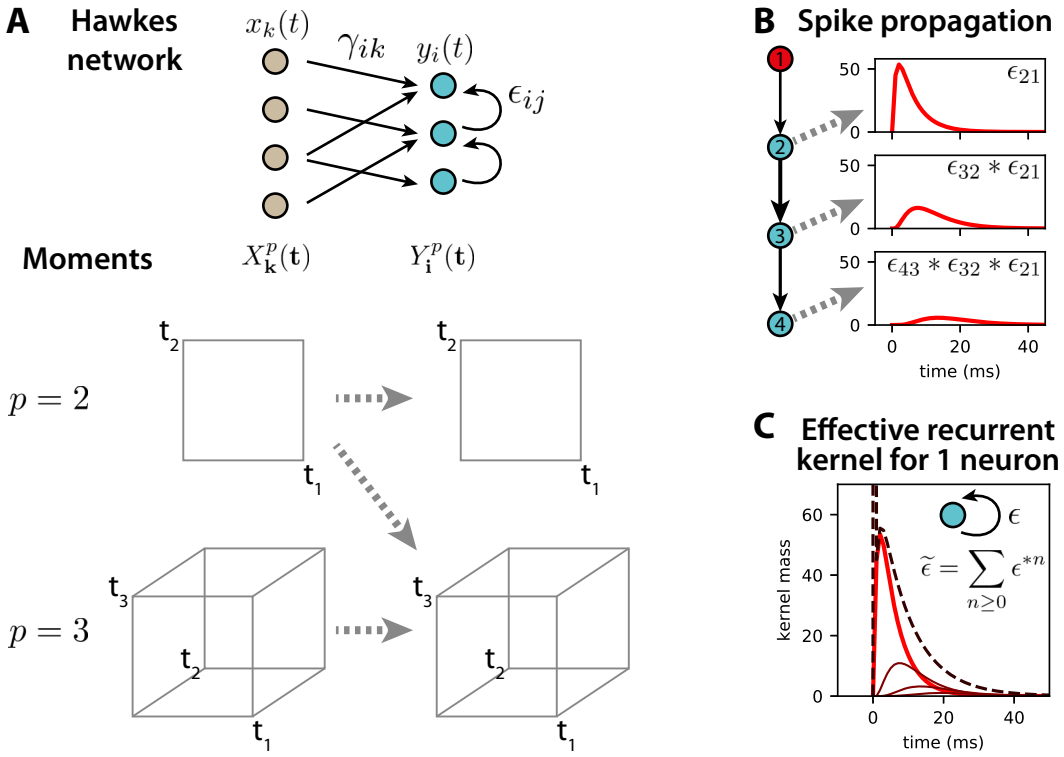

Figure 1: **Overview of the present study.** This schematic diagram presents the goal of this work, which is the characterization of the mapping between the moments of the input and output spike trains (i.e., their correlation structure) for a multivariate Hawkes process. In the present paper we refer to it as a Hawkes network, where nodes are the individual neurons that emit (or fire) spikes, borrowing terminology from neuroscience. The afferent and recurrent connectivity are described by the kernel functions γ_{ik} and ϵ_{ij}, respectively. The matrices and cubes represent the second- and third-order moments, which are formally tensors with "spatial" coordinates (over neurons) and temporal variables. Note that the difference between space and time here is simply their discrete and continuous natures. Dashed gray arrows represent cross-order contributions from the input to the output moments. **B:** This diagram depicts the response of the downstream neurons due to a spike fired by the red neuron. The red curves represent the increase of firing rate following the spikes, which is given by the convolution of the synaptic kernels ϵ_{ij}. **C:** Similar diagram to panel B for a neuron with a self-connection with kernel ϵ (thick bright red curve). The effective recurrent kernel $\widetilde{\epsilon}$ (dashed dark red curve) is given by the superposition of the self-convolutions of ϵ (thin solid red curves in addition to the thick one). It corresponds to the Green function of the network in the context of linear dynamics.

a network (output) population of n neurons denoted by $y(t) = (y_1(t), \cdots, y_n(t))$ which are also a superposition of Dirac deltas.

Definition 1 (Hawkes Process) *The Hawkes process is a point-emission process whose intensity $\nu(t) = (\nu_1(t), \cdots, \nu_n(t))$ depends upon both the past input spiking activity $x(u)$ and its own past spiking activity $y(u)$ with $u < t$ as well as on a time-dependent (possibly stochastic) rate $\lambda : \mathbb{R} \to \mathbb{R}_+^n$:*

$$\nu_i(t) = \lambda_i(t) + (\epsilon_{ij} * y_j)(t) + (\gamma_{ik} * x_k)(t) \ , \tag{1}$$

where $\gamma = \{\gamma_{ik}\}_{i,k=1}^{n,m} : \mathbb{R} \to \mathbb{R}_+^{n \times m}$ is a matrix of "synaptic" kernels, made of functions $\gamma_{ik} : \mathbb{R} \to \mathbb{R}_+$ that describe the causal effect from the input neuron x_k on the network neuron y_i. These functions are equal to zero for all $t \leq 0$. Similarly $\epsilon = \{\epsilon_{ij}\}_{i,j=1}^{n,n} : \mathbb{R} \to \mathbb{R}_+^{n \times n}$ is a matrix of kernels $\epsilon_{ij} : \mathbb{R} \to \mathbb{R}_+$, each corresponding to the recurrent interraction from neuron y_j to neuron y_i. Note that the convolution operator $*$ is a matrix convolution; see Eq. (5) below. In this paper we omit the summation symbol in line with Einstein's convention for tensor calculus. All kernel functions and spontaneous rate functions are assumed to be positive-valued.
Let $N_i(t) = \int_0^t y_i(u)\mathrm{d}u$ be the counting process associated with the spiking activity $y_i(t)$, which gives the number of spikes from 0 to t for the network neuron i. The increment of the i^{th} counting process $N_i(t)$ in an infinitesimally small bin size $\mathrm{d}t$ is given by

$$\mathrm{d}N_i(t) \sim \text{Poisson}\big(\nu_i(t)\mathrm{d}t\big) \tag{2}$$

As a consequence, we have $\langle dN_i(t) \rangle = \nu_i(t)dt$, hence $\langle y_i(t) \rangle = \langle dN_i(t)/\mathrm{d}t \rangle = \nu_i(t)$.

Remark 1 (Atomic contributions and contraction of indices) *Note that for an infinitesimally small $\mathrm{d}t$, the increment $\mathrm{d}N_i(t)$ can take only 2 values: 0 or 1. In that case, we have for any $p \in \mathbb{N}_+$,*

$$(\mathrm{d}N_i(t))^p = \mathrm{d}N_i(t) \tag{3}$$

Following, atomic contributions arise from the point-process nature of spike trains when taking expectations of products of $y_i(t)$ for all possible redundancies in the time variables together with the "spatial" coordinates (Daley and Vere-Jones 1988). For the example of the 2nd-order moment, it corresponds to the twofold condition $k_1 = k_2$ and $t_1 = t_2$, which leads to the second term in

$$\langle x_{k_1}(t_1) x_{k_2}(t_2) \rangle = \langle x_{k_1}(t_1) \rangle \langle x_{k_2}(t_2) \rangle + \langle x_{k_1}(t_1) \rangle \ \delta_{k_1 k_2} \delta(t_2 - t_1) \ . \tag{4}$$

In the remainder we refer to terms involving Kronecker deltas $\delta_{k_1 k_2}$ and Dirac delta $\delta(t_2 - t_1)$ as contractions of indices (here 1 and 2).

Definition 2 (Matrix convolution) *In Eq. (1), the standard convolution is extended to a matrix form, which involves a matrix multiplication. For the kernel matrix ϵ and vector y, the i^{th} element of the matrix convolution is given by*

$$(\epsilon_{ij} * y_j)(t) \equiv \sum_{j=1}^{n} \int_0^\infty \epsilon_{ij}(u) y_j(t-u) \mathrm{d}u \ . \tag{5}$$

Definition 3 (Moments of order p) *Let $\mathbf{k} = (k_1, \cdots, k_p)$ denote a set of p coordinates $k_r \in I_m = \{1, \cdots, m\}$. The moment of order p of the input population evaluated at times $\mathbf{t} = (t_1, \cdots, t_p)$ is defined as*

$$X^p_{\mathbf{k}}(\mathbf{t}) \equiv \left\langle \prod_{r=1}^{p} x_{k_r}(t_r) \right\rangle_x \ . \tag{6}$$

Similarly, the moment of order p of the output population for the coordinates $\mathbf{i} = (i_1, \cdots, i_p) \in I_n^p$ and the time variables $\mathbf{t} = (t_1, \cdots, t_p)$ is defined as

$$Y_{\mathbf{i}}^p(\mathbf{t}) \equiv \left\langle \prod_{r=1}^{p} y_{i_r}(t_r) \right\rangle_{y,x,\lambda} . \tag{7}$$

Note that the mathematical expectation corresponds to three sources of stochasticity, as indicated by the superscript. Note that, due to the recurrent connectivity, the dependency of y on itself also concerns the past activity.

Remark 2 (Symmetry of moments) *The moments $X_{\mathbf{k}}^p(\mathbf{t})$ and $Y_{\mathbf{i}}^p(\mathbf{t})$ have many symmetries. For the example of the input moments, any permutation Π of I_p such that the transformed coordinates $\Pi(\mathbf{k}) = (k_{\Pi(1)}, \cdots, k_{\Pi(p)})$ and $\Pi(\mathbf{t}) = (t_{\Pi(1)}, \cdots, t_{\Pi(p)})$ leaves $X_{\mathbf{k}}^p(\mathbf{t})$ invariant:*

$$X_{\Pi(\mathbf{k})}^p\big(\Pi(\mathbf{t})\big) = X_{\mathbf{k}}^p(\mathbf{t}) . \tag{8}$$

Definition 4 (Generalized Spatio-Temporal Delta Function) *Let $\delta_{\mathbf{k}}(\mathbf{t})$ be the generalized delta function defined for the set of coordinates $\mathbf{k} = (k_1, \cdots, k_p)$ and times $\mathbf{t} = (t_1, \cdots, t_p)$, which combines the Kronecker and Dirac delta functions as*

$$\delta_{\mathbf{k}}(\mathbf{t}) = \begin{cases} 1 & \text{if } p \in \{0, 1\} , \\ \prod_{r=2}^{p} \delta\left(t_{r-1} - t_r\right) & \text{if } k_1 = \cdots = k_p \text{ and } t_1 = \cdots = t_p \text{ with } p \geq 2 , \\ 0 & \text{otherwise.} \end{cases} \tag{9}$$

Note that for $p = 2$, one recovers the product of the standard Kronecker delta with the Dirac delta: $\delta_{k_1,k_2}(t_1, t_2) = \delta_{k_1,k_2}\delta(t_1 - t_2)$. Note also that when the lower index $\mathbf{k}$ is omitted, we will assume that $k_1 = \cdots = k_p$ (i.e. single neuron case).

Example 1 (Moment for a single spike train with oscillatory firing rate) *Before presenting the general result, we provide an illustrative example to fix ideas and help the reader with concepts and notation.*

Case $p = 2$:

For a single (input) neuron driven by a deterministic rate function μ, the contraction in the 2nd-order moment corresponds to the condition $t_1 = t_2$ without "spatial" coordinates here, simplifying Eq. (4):

$$\langle x(t_1)x(t_2)\rangle_x = \mu(t_1)\mu(t_2) + \mu(t_1)\,\delta(t_2 - t_1) . \tag{10}$$

Case $p = 3$:

The 3rd-order moment for a single spike train is given by

$$\begin{aligned} \langle x(t_1)x(t_2)x(t_3)\rangle_x \;=\; & \mu(t_1)\mu(t_2)\mu(t_3) + \mu(t_1)\delta(t_2 - t_1)\mu(t_3) + \delta(t_1 - t_3)\mu(t_1)\mu(t_2) \\ & + \mu(t_1)\mu(t_2)\delta(t_3 - t_2) + \mu(t_1)\delta(t_2 - t_1)\delta(t_3 - t_1) . \end{aligned} \tag{11}$$

This expression exhibits two "extreme" cases where all time variables are equal $t_1 = t_2 = t_3$ corresponding to the two Dirac delta $\delta(t_2 - t_1)\delta(t_3 - t_1) = \delta(t_1, t_2, t_3)$ for the partition $\big\{\{1, 2, 3\}\big\}$, and where they are all distinct giving $\mu(t_1)\mu(t_2)\mu(t_3)$ for $\big\{\{1\}, \{2\}, \{3\}\big\}$. In addition, the three remaining terms involve a contraction for 2 out of the 3 variables.

Numerical simulation:

Fig. 2 illustrates the moments for $p = 2$ and 3 with a single spike train driven by an oscillatory firing rate. Note that "spatial" coordinates $\mathbf{k}$ in the above equation are simply ignored, together with the Kronecker deltas. Fig. 2B, C and E highlight the atomic contributions along the various "diagonals" where the time variables coincide. Away from those subspaces, the spike densities are much lower, as can be seen in the scaling of values in the middle and right plots of Fig. 2C and E. Note that the main diagonal for $p = 3$ is slightly larger than that for $p = 2$, as autocorrelation effects cumulate.

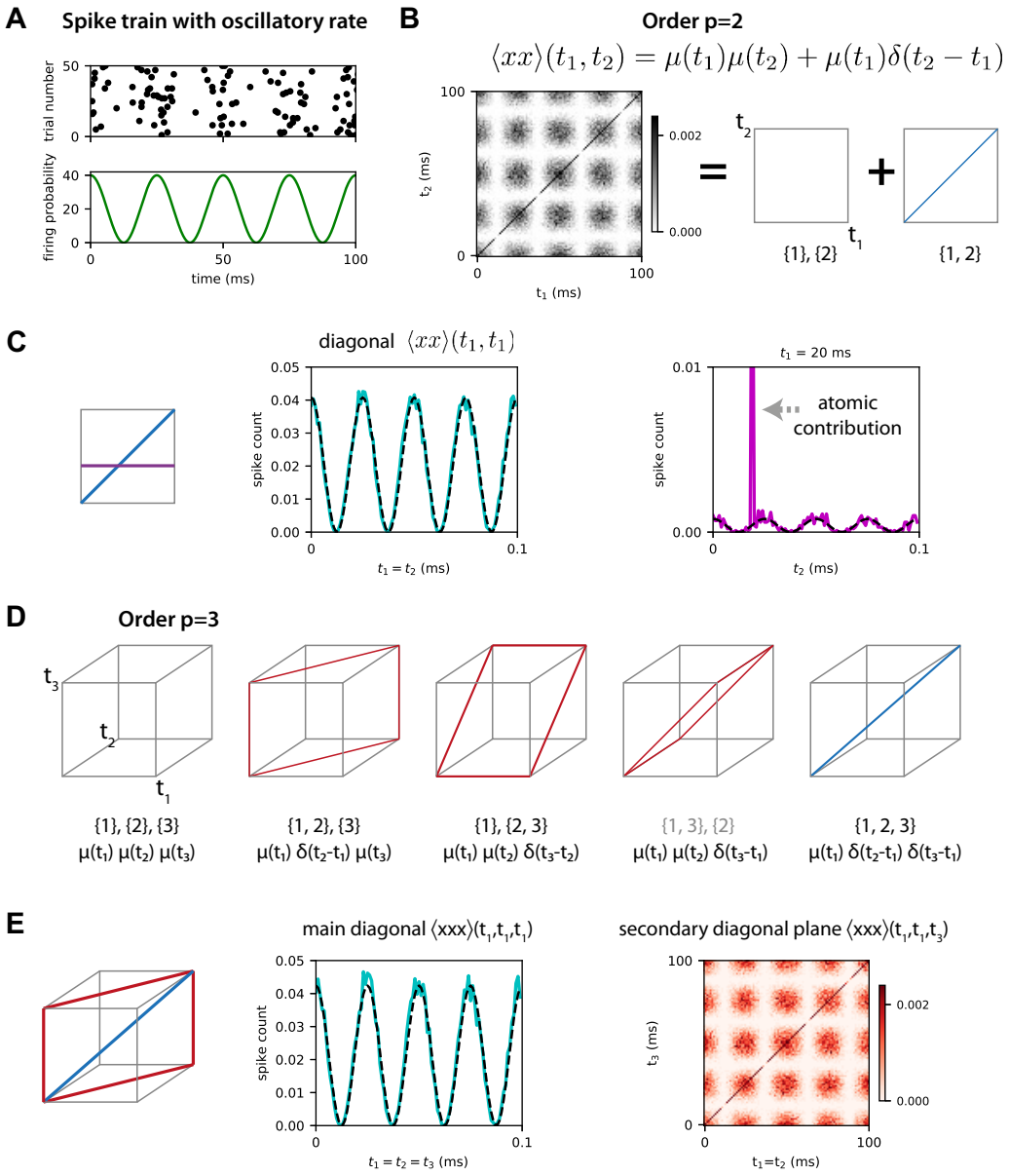

Figure 2: **Input moments for a spike train. A:** Spike raster (top plot) for 50 simulations using an oscillatory rate function (bottom plot). **B:** 2nd-order moment (left plot) averaged over 10000 simulations, where darker pixels indicate a higher spike density. The middle and right diagrams illustrate the decomposition into a contribution due to rate correlation (co-fluctuations) and to atomic contributions (diagonal in cyan), respectively. Each contribution corresponds to a partition of $I_2 = \{1, 2\}$, as indicated below. **C:** Example slices of the matrix as indicated in the left diagram for a fixed t_1 (middle plot) and along the diagonal (right plot). Note the difference in scaling for the y-axis (1 order of magnitude). **D:** Decomposition of the 3rd-order moment using the partitions of $I_3 = \{1, 2, 3\}$, similar to panel B. **E:** Main diagonal of the 3rd-order moment corresponding to $t_1 = t_2 = t_3$ and a plane corresponding to $t_1 = t_2$, see the blue line and red plane in the left schematic diagram (color coded). All prediction curves are calculated using Eq. (12).

Proposition 1 (Moments for inputs driven by deterministic rate functions) *Let $\mathcal{P}_p = \mathcal{P}(I_p)$ denote the set of all partitions Φ of the set $I_p = \{1, \cdots, p\}$. If each input neuron is independent from each other and the firing rate of neuron $x_k(t)$ is given by $\mu_k(t)$, then the input moment of order p over the coordinates $\mathbf{k} = (k_1, \cdots, k_p)$ at times $\mathbf{t} = (t_1, \cdots, t_p)$ can be expressed as*

$$X^p_{\mathbf{k}}(\mathbf{t}) = \sum_{\Phi \in \mathcal{P}_p} \prod_{S \in \Phi} \delta_{\mathbf{k}_S}(\mathbf{t}_S)\ \mu_{k_{\check{S}}}(t_{\check{S}})\ , \tag{12}$$

where S spans the disjoint subsets of Φ whose union is I_p, with $\mathbf{k}_S = \{k_r, r \in S\}$ and $\mathbf{t}_S = \{t_r, r \in S\}$. In addition, the instantaneous firing rate appears with a representative index, here taken as the minimum $\check{S} = \min(S)$. Recall the convention $\delta_{\mathbf{k}_S}(\mathbf{t}_S) = 1$ when S is a singleton.

Remark 3 *The grouping of indices from a given subset S in Eq.* (12) *is a direct consequence of the* contraction *highlighted in remark 1, resulting in an* atomic contribution *where the paired spatial coordinates and temporal variables related to S are involved in the generalized delta function δ.*

Proof of Proposition 1: Eq. (12) can be obtained using the moment generating function (Daley and Vere-Jones 1988; Ocker, Josić, Shea-Brown, and Buice 2017), via its p^{th} derivative for order p. Here we provide a proof by induction, which highlights the key observation that every combination of contractions can be described by a partition.
Let assume that Eq. (12) is valid for all orders $2 \leq p' \leq p-1$. Now considering the order p with given coordinates $\mathbf{k}$ and time variables $\mathbf{t}$ in $X_{\mathbf{k}}(\mathbf{t})$, we denote by S^* the set of order indices in I_{p-1} such that coordinates and times are identical to their counterpart for p, namely $S^* = \{r \in I_{p-1}, k_r = k_p \text{ and } t_r = t_p\}$. Using the probabilistic independence as before, we can write:

$$\begin{aligned}
X_{\mathbf{k}}(\mathbf{t}) &= \left\langle \prod_{r \in I_p \setminus S^*} x_{k_r}(t_r) \right\rangle \left\langle \prod_{r \in S^*} x_{k_r}(t_r) \right\rangle \\
&= \left(\sum_{\Phi' \in \mathcal{P}(I_p \setminus S^*)} \prod_{S \in \Phi'} \delta_{\mathbf{k}_S}(\mathbf{t}_S)\ \mu_{k_{\check{S}}}(t_{\check{S}}) \right) \delta_{\mathbf{k}_{S^*}}(\mathbf{t}_{S^*})\ \mu_{k_{\check{S}^*}}(t_{\check{S}^*}) \\
&= \sum_{\substack{\Phi = \Phi' \cup \{S^*\} \\ \Phi' \in \mathcal{P}(I_p \setminus S^*)}} \prod_{S \in \Phi} \delta_{\mathbf{k}_S}(\mathbf{t}_S)\ \mu_{k_{\check{S}}}(t_{\check{S}})\ .
\end{aligned} \tag{13}$$

In the second line, we have used the hypothesis for order $p - |S^*|$ where $|S^*|$ is the number of elements in S^* for the indices that are not in S^*, as well as the contraction for all elements in S^*. The previous expression is valid for each $S^* \subset I_p$ containing p, which is determined by $\mathbf{k}$ and $\mathbf{t}$. We conclude by observing that the above dichotomy of partitions Φ actually spans the whole set $\mathcal{P}(I_p) = \mathcal{P}_p$:

$$\bigcup_{\substack{S^* \subset I_p \\ S^* \ni p}} \bigcup_{\Phi' \in \mathcal{P}(I_p \setminus S^*)} \Phi' \cup \{S^*\} = \mathcal{P}(I_p)\ , \tag{14}$$

which accounts for all possible configurations of $\mathbf{k}$ and $\mathbf{t}$. This is also related to the decomposition of the Bell number —giving the number of partitions $\Phi \in \mathcal{P}_p$— in the sum of the Stirling numbers of the second kind $s_{p,q}$ —giving the number of partitions Φ that have q groups. They satisfy the relationship $s_{p,q} = s_{p-1,q-1} + q s_{p-1,q}$ for all $2 \leq q \leq p-1$ (corresponding to the above dichotomy), as well as the "boundary" condition $s_{p,q} = 1$ when $q = 1$ or $q = p$. □

2.1 Network with afferent connectivity

Now that we have introduced definitions and concepts that will be useful to characterize the high-order moments, we turn to the case of a network with afferent connections, but no recurrent connections. The following theorem is the first of our two core results. We denote the driving rate function of the network neurons that lumps together the spontaneous activity and the input influx by

$$\nu_i^{\epsilon=0}(t) = \lambda_i(t) + (\gamma_{ik} * x_k)(t) \ . \tag{15}$$

Definition 5 (Moment for the input rate λ) *Considering the stochastic spontaneous rate function λ (e.g., a Cox process), we define the corresponding moment of order p for the coordinates $\mathbf{i} \in I_n^p$ at times $\mathbf{t} = (t_1, \cdots, t_p)$ as*

$$\Lambda_{\mathbf{i}}^p(\mathbf{t}) \equiv \left\langle \prod_{r=1}^{p} \lambda_{i_r}(t_r) \right\rangle_{\lambda} \ . \tag{16}$$

Definition 6 (Tensor convolution operator) *Let $\alpha_{ij} : \mathbb{R} \to \mathbb{R}^{n,m}$ be a matrix of kernels. We define the $2p$-dimensional tensor that replicates the matrix α for all pairs of indices $(i_r j_r)$:*

$$\boldsymbol{\alpha}_{\mathbf{ij}}^p(\mathbf{t}) = \prod_{r=1}^{p} \alpha_{i_r j_r}(t_r) \tag{17}$$

with $\mathbf{i} = (i_1, \cdots, i_p) \in I_n^p$, $\mathbf{j} = (j_1, \cdots, j_p) \in I_m^p$ and $\mathbf{t} = (t_1, \cdots, t_p)$. For a p-order tensor $T_{\mathbf{j}}^p$ with coordinates $\mathbf{j}$, the tensor convolution $\circledast$ between $\boldsymbol{\alpha}_{\mathbf{ij}}^p$ and $X_{\mathbf{j}}$ evaluated at times $\mathbf{t}$ gives the following tensor of oreder p:

$$\begin{aligned} \left(\boldsymbol{\alpha}_{\mathbf{ij}}^p \circledast T_{\mathbf{j}}^p\right)(\mathbf{t}) &\equiv \sum_{\mathbf{j}=(j_1,\cdots,j_p)} \int_{\mathbf{u}\in\mathbb{R}^p} \boldsymbol{\alpha}_{\mathbf{ij}}^p(\mathbf{u}) T_{\mathbf{j}}^p(\mathbf{t}-\mathbf{u}) \mathrm{d}\mathbf{u} \\ &= \left(\alpha_{i_1 j_1} \overset{1}{*} \cdots \alpha_{i_p j_p} \overset{p}{*} T_{j_1,\cdots,j_p}^p\right)(\mathbf{t}) \ . \end{aligned} \tag{18}$$

The second line is a reformulation to stress that the convolutions of α are applied on each of the p dimensions —as indicated above each asterisk— on the tensor T^p, followed by the summation for the tensor product (similar to a matrix product), in line with the definition in Eq. (5).

In essence, this convolution operator involves the same joint "multiplication" on paired spatial and temporal dimensions (related to k_i and t_i, the temporal convolution being seen as a function multiplication operator) as the matrix convolution in Eq. (5), but extended on all dimensions of the tensor. In particular, this operation is linear.

Definition 7 (Moment for the filtered inputs) *As with the spontaneous rate λ, we define the following moments of the input x filtered by the afferent kernels γ:*

$$\Gamma_{\mathbf{i}}^p(\mathbf{t}) \equiv \left(\boldsymbol{\gamma}_{\mathbf{ik}}^p \circledast X_{\mathbf{k}}^p\right)(\mathbf{t}) \ , \tag{19}$$

with $\mathbf{i} = (i_1, \cdots, i_p) \in I_n^p$, $\mathbf{k} = (k_1, \cdots, k_p) \in I_m^p$ and $\mathbf{t} = (t_1, \cdots, t_p)$.

Note that this definition implicitly involves the averaging over the statistics of the inputs x, that is $\langle \cdots \rangle_x$.

Definition 8 (Moment symmetrical expansion operator) *Let us consider two tensors of order q and r, say $T_{\mathbf{j}'}^q(\mathbf{t}')$ with coordinates $\mathbf{j}' = (j_1', \cdots j_q')$ and $\mathbf{t}' = (t_1', \cdots t_q')$ as well as $U_{\mathbf{j}''}^r(\mathbf{t}'')$ with coordinates $\mathbf{j}'' = (j_1'', \cdots j_q'')$ and $\mathbf{t}'' = (t_1'', \cdots t_r'')$. For any given $p \geq q + r$, we*

define the following tensor operation that constructs a moment of order p with $\mathbf{i} = (i_1, \cdots, i_p)$ and $\mathbf{t} = (t_1, \cdots, t_p)$ from the tensors T and U of smaller orders q and r:

$$\mathcal{A}^p[T^q, U^r]_{\mathbf{i}}(\mathbf{t}) \equiv \sum_{\substack{A\subset I_p, B\subset I_p \\ |A|=q, |B|=r \\ A\cap B=\emptyset}} \sum_{\substack{\Phi\in\mathcal{P}_p \\ \check{\Phi}=A\cup B}} \left(\prod_{S\in\Phi} \delta_{\mathbf{i}_S}(\mathbf{t}_S) \right) T^q_{\mathbf{i}_A}(\mathbf{t}_A)\, U^r_{\mathbf{i}_B}(\mathbf{t}_B) \ . \tag{20}$$

Here we have defined $\check{\Phi} = \{\check{S}, S \in \Phi\}$, the set of minima for the groups in the partition Φ. By convention, the 0-order tensors are valued 1 when A or $B = \emptyset$.

Eq. (20) uses contractions to augment the order of the combinations of tensors T^q and U^r from $q + r$ to p with all possible symmetries. In particular, if T^q and U^r are symmetric tensors (see Remark 2) with respect to all their own dimensions, the output of $\mathcal{A}^p$ is symmetric as well.

Theorem 1 (Input-output mapping for afferent connectivity) *Consider an uncoupled Hawkes network (definition 1) whose neurons are excited by both inputs x (via afferent connections) and spontaneous rate λ, which are probabilistically independent. The moment $M^{y,\epsilon=0}_{\mathbf{i}}$ of order p of of the network population depends on all smaller-order moments X^q of the input population as well as moments for the spontaneous firing rate Λ^r:*

$$Y^{p,\epsilon=0}_{\mathbf{i}}(\mathbf{t}) = \sum_{0\le q+r\le p} \mathcal{A}^p \left[\Gamma^q, \Lambda^r\right]_{\mathbf{i}}(\mathbf{t}) \ , \tag{21}$$

where the moments Γ and Λ are defined in Eqs. (16) *and* (19)*, respectively. Note that the superscript of the moment corresponds to the situation where the network population is decoupled (i.e., $\epsilon = 0$).*

Proof of Theorem 1: Provided the statistics of inputs x and the spontaneous rate λ is known, the spiking activity of the network neurons is determined by the driving rate function $\nu^{\epsilon=0}_i$ in Eq. (15). Similar to Eq. (12) in Proposition 1, the Poisson nature of the spiking of the network neurons thus gives the following expression for the unconnected neurons with spike trains y:

$$\begin{aligned}
Y^{p,\epsilon=0}_{\mathbf{i}}(\mathbf{t}) &= \left\langle \prod_{r=1}^{p} y_{i_r}(t_r) \right\rangle_{y,x,\lambda} \\
&= \left\langle \sum_{\Phi\in\mathcal{P}_p} \prod_{S\in\Phi} \delta_{\mathbf{i}_S}(\mathbf{t}_S) \nu^{\epsilon=0}_{i_{\check{S}}}(t_{\check{S}}) \right\rangle_{x,\lambda} \\
&= \sum_{\Phi\in\mathcal{P}_p} \left(\prod_{S\in\Phi} \delta_{\mathbf{i}_S}(\mathbf{t}_S) \right) \left\langle \prod_{S\in\Phi} \nu^{\epsilon=0}_{i_{\check{S}}}(t_{\check{S}}) \right\rangle_{x,\lambda} \\
&= \sum_{\Phi\in\mathcal{P}_p} \left(\prod_{S\in\Phi} \delta_{\mathbf{i}_S}(\mathbf{t}_S) \right) \left\langle \prod_{r\in\check{\Phi}} \left(\lambda_{i_r}(t_r) + (\gamma_{i_r k} * x_k)(t_r)\right) \right\rangle_{x,\lambda} \ .
\end{aligned} \tag{22}$$

In the previous expression, the contractions basically extend the moment of smaller order $|\check{\Phi}| \le p$ for the driving rate $\nu^{\epsilon=0}$ to the order p.
The product involving the sum of $\lambda_{i_{\check{S}}} + \gamma_{i_{\check{S}}k} * x_k$ gives $2^{|\check{\Phi}|}$ terms with $|\check{\Phi}|$ being the number of elements in $\check{\Phi}$. Now we develop this product to isolate the contributions originating from the input moments of the same order, as well as with the spontaneous rate. To this end, we

define $A \subset I_p$ the subset of indices belonging to $\check{\Phi}$ that concern input neurons in Eq. (22), while $B = \check{\Phi} \setminus A$ is the subset of indices that concern λ. This gives

$$\begin{aligned} Y_{\mathbf{i}}^{p,\epsilon=0}(\mathbf{t}) &= \sum_{\Phi\in\mathcal{P}_p} \left(\prod_{S\in\Phi} \delta_{\mathbf{i}_S}(\mathbf{t}_S)\right) \sum_{\substack{A\cup B=\check{\Phi}\\ A\cap B=\emptyset}} \left\langle \prod_{r\in A} (\gamma_{i_r k} * x_k)(t_r) \right\rangle_x \left\langle \prod_{r'\in B} \lambda_{i_{r'}}(t_{r'}) \right\rangle_\lambda \\ &= \sum_{\Phi\in\mathcal{P}_p} \left(\prod_{S\in\Phi} \delta_{\mathbf{i}_S}(\mathbf{t}_S)\right) \sum_{\substack{A\cup B=\check{\Phi}\\ A\cap B=\emptyset}} \Gamma_{\mathbf{i}_A}^{|A|}(\mathbf{t}_A)\ \Lambda_{\mathbf{i}_B}^{|B|}(\mathbf{t}_B) \\ &= \sum_{\substack{A\subset I_p, B\subset I_p\\ A\cap B=\emptyset}} \sum_{\substack{\Phi\in\mathcal{P}_p\\ \check{\Phi}=A\cup B}} \left(\prod_{S\in\Phi} \delta_{\mathbf{i}_S}(\mathbf{t}_S)\right) \Gamma_{\mathbf{i}_A}^{|A|}(\mathbf{t}_A)\ \Lambda_{\mathbf{i}_B}^{|B|}(\mathbf{t}_B)\ . \end{aligned} \tag{23}$$

From the second line to the last line, we have swapped the summation terms of the partitions Φ and the decomposition of $\check{\Phi}$ in two subsets. The important point here is to understand that the construction of $\check{\Phi}$ from A and B exactly spans the whole set of partitions $\mathcal{P}_p$. Note that A and B can be empty sets. Finally, we simply group the subsets A of the same size q, and similarly B of the same size r:

$$Y_{\mathbf{i}}^{p,\epsilon=0}(\mathbf{t}) = \sum_{0\le q+r\le p} \sum_{\substack{A\subset I_p, B\subset I_p\\ |A|=q, |B|=r\\ A\cap B=\emptyset}} \sum_{\substack{\Phi\in\mathcal{P}_p\\ \check{\Phi}=A\cup B}} \left(\prod_{S\in\Phi} \delta_{\mathbf{i}_S}(\mathbf{t}_S)\right) \Gamma_{\mathbf{i}_A}^{q}(\mathbf{t}_A)\ \Lambda_{\mathbf{i}_B}^{r}(\mathbf{t}_B)\ , \tag{24}$$

which gives Eq. (21) after using the expression for the operator $\mathcal{A}^p$ in Eq. (20). □

Remark 4 *When the network of unconnected neurons is not driven by an spontaneous rate ($\lambda = 0$), the moment expansion operator in Eq.* (20) *can be simplified with $U = 0$ as*

$$\mathcal{A}^p[T^q, 0]_{\mathbf{i}}(\mathbf{t}) = \sum_{\substack{A\subset I_p\\ |A|=q}} \sum_{\substack{\Phi\in\mathcal{P}_p\\ \check{\Phi}=A}} \left(\prod_{S\in\Phi} \delta_{\mathbf{i}_S}(\mathbf{t}_S)\right)\ T_{\mathbf{i}_A}^q(\mathbf{t}_A)\ , \tag{25}$$

which means that

$$\begin{aligned} Y_{\mathbf{i}}^{p,\epsilon=0}(\mathbf{t}) &= \sum_{q=0}^{p} \mathcal{A}^p\left[\Gamma^q, 0\right]_{\mathbf{i}}(\mathbf{t}) \\ &= \sum_{\Phi\in\mathcal{P}_p} \left(\prod_{S\in\Phi} \delta_{\mathbf{i}_S}(\mathbf{t}_S)\right) \Gamma_{\mathbf{i}_{\check{\Phi}}}^{|\check{\Phi}|}(\mathbf{t}_{\check{\Phi}}) \end{aligned} \tag{26}$$

Conversely, in the absence of spiking inputs ($\gamma = 0$) and when the driving rates $\lambda_i(t)$ are deterministic, the moments Λ simply come from the multiplication of the rate functions:

$$Y_{\mathbf{i}}^{p,\epsilon=0}(\mathbf{t}) = \sum_{\Phi\in\mathcal{P}_p} \prod_{S\in\Phi} \left[\delta_{\mathbf{i}_S}(\mathbf{t}_S)\lambda_{\mathbf{i}_{\check{S}}}(\mathbf{t}_{\check{S}})\right]\ . \tag{27}$$

2.2 Network with recurrent connectivity

The last step is to consider connections determined by ϵ between the network neurons, the second half of our core result.

Definition 9 (Effective recurrent kernel) *Let $\widetilde{\epsilon} : \mathbb{R} \to \mathbb{R}^{n\times n}$ denote the effective recurrent kernel and be defined as*

$$\widetilde{\epsilon}_{ij}(t) = \sum_{n\geq 0} \epsilon_{ij}^{*n}(t) \tag{28}$$

where

$$\epsilon_{ij}^{*n}(t) = \begin{cases} \left(\epsilon_{il}^{*(n-1)} * \epsilon_{lj}\right)(t) & \text{if} \quad n > 0 \\ \delta_{ij}(t,0) & \text{if} \quad n = 0 \end{cases} \tag{29}$$

is the n^{th} order convolution.

Recall that the convolution is defined for kernel matrices, see Eq. (5). Because $\epsilon_{ij}(t) = 0$ for $t \leq 0$ and all pairs (i, j) (due to the causality requirement), $\widetilde{\epsilon}_{ij}(t) = 0$ as well for $t \leq 0$.

Property 1 *The effective recurrent kernel $\widetilde{\epsilon}$ satisfies the following self-consistency equation:*

$$\left(\kappa * \widetilde{\epsilon}\right)_{ij}(t) = \delta_{ij}(t,0) \ , \tag{30}$$

where $\kappa_{ij}(t) \equiv \delta_{ij}(t,0) - \epsilon_{ij}(t)$. Therefore, $\widetilde{\epsilon}$ can be thought as the inverse of κ for the convolution operator.

Proof of Property 1: By convolving the ϵ kernel with the effective recurrent kernel $\widetilde{\epsilon}$, we find (omitting the time variables)

$$\left(\epsilon * \widetilde{\epsilon}\right)_{ij} = \epsilon_{ik} * \left(\sum_{n\geq 0} \epsilon_{kj}^{*n}\right) = \sum_{n\geq 1} \epsilon_{ij}^{*n} = \widetilde{\epsilon}_{ij} - \delta_{ij} \ , \tag{31}$$

which we reorganize to factorize $\widetilde{\epsilon}$, obtaining Eq. (30). □

Example 2 (Single neuron with self-connection and with spontaneous rate λ) *We firstly present an illustrative version of our proof by induction for a single neuron with self-feedback and driven by a deterministic rate λ in the cases $1 \leq p \leq 3$. In this example $\langle \cdots \rangle = \langle \cdots \rangle_y$ as there is no other source of stochasticity. Note that $p = 2$ corresponds to Hawkes' results (Hawkes 1971a) with moments instead of (auto)covariances. The motivation is providing a concrete case for stepping from orders p to $p + 1$, which is formalized in the proof below.*
Cases $p = 1$ and $p = 2$:
The first-order moment for $p = 1$ corresponds to the mean firing rate and can be calculated from the spontaneous rate function λ by solving the self-consistency equation given by the second line of Eq. (1) *using the equality for the instantaneous firing rate $\langle y(t)\rangle = \langle \nu(t)\rangle$:*

$$\langle y(t)\rangle = \left(\widetilde{\epsilon} * \lambda\right)(t) \ . \tag{32}$$

For the second order, the point is to take into account the effects of spikes upon the future spiking probability, with the effect of the self-feedback loop. Assuming $t_1 \leq t_2$ (purple semi-plane in Fig. 3A), we can develop $y(t_2)$ in $\langle yy\rangle(t_1, t_2)$ using Eq. (1)*. This holds because the rate function $\nu(t_2)$ requires the knowledge of past spiking activity $y(u)$ with $u < t_2$, as illustrated by the blue arrow in Fig. 3A, moving toward the diagonal $t_1 = t_2$. This development gives*

$$\begin{aligned} \langle yy\rangle(t_1,t_2) &= \langle y(t_1)\nu(t_2)\rangle + \langle y(t_1)\rangle\delta(t_2 - t_1) \\ &= \langle y(t_1)[\epsilon * y](t_2)\rangle + \langle y(t_1)\rangle\lambda(t_2) + \langle y(t_1)\rangle\delta(t_2 - t_1) \\ &= [\epsilon \overset{2}{*} \overline{\langle yy\rangle}](t_1,t_2) + \overline{\langle y\rangle\lambda}(t_1,t_2) + \overline{\langle y\rangle\delta^{21}}(t_1,t_2) \ . \end{aligned} \tag{33}$$

Note that ν is inside the angular brackets on the right-hand side of the first line, because $\nu(t_2)$ and $y(t_1)$ are not independent, when the difference in the time variables lies within the range

of $\widetilde{\epsilon}$. The last line is simply a rewriting using a specific notation with a line above multivariate functions to indicate the order of the functions with respect to the time variables, which will be useful for this example. In addition, we use the notation introduce in Eq. (18) *where $\overset{2}{*}$ indicates the convolution performed on the second time variable t_2 and the Dirac delta $\delta^{21}(t_2) := \delta(t_2 - t_1)$ is a redundant expression as a function of t_2, while keeping the information about t_1.*
The solution $\langle yy\rangle(t_1, t_2)$ must satisfy Eq. (33) *for all $t_1 \leq t_2$, which is a Wiener-Hopf equation. The atomic contribution (Dirac delta) acts as a "boundary condition" when $t_2 \to t_1$. Our strategy is the following: we propose a solution for the moment of order $p = 2$ and verify that it satisfies the required Eq.* (33)*. As the solution is fully symmetric in t_1 and t_2, this implies that the solution is also valid on the complementary space $t_2 \leq t_1$, being eventually valid for all $(t_1, t_2) \in \mathbb{R}^2$. The putative 2nd-order moment is:*

$$\overline{\langle yy\rangle}(t_1, t_2) = \left[\widetilde{\epsilon} \overset{1}{*} \widetilde{\epsilon} \overset{2}{*} (\overline{\lambda\lambda} + \overline{\lambda\delta^{21}})\right](t_1, t_2) \ , \tag{34}$$

Note that our notation does not require the time variables, allowing for compact writing. We use the equality in Eq. (30) *on $\widetilde{\epsilon}\overset{2}{*}$ to obtain*

$$\begin{aligned} \overline{\langle yy\rangle} &= \widetilde{\epsilon} \overset{1}{*} (\epsilon * \widetilde{\epsilon} + \delta) \overset{2}{*} (\overline{\lambda\lambda} + \overline{\lambda\delta^{21}}) \\ &= \epsilon \overset{2}{*} \overline{\langle yy\rangle} + \widetilde{\epsilon} \overset{1}{*} \overline{\lambda\lambda} + \widetilde{\epsilon} \overset{1}{*} \overline{\lambda\delta^{21}} \ . \end{aligned} \tag{35}$$

For the first term of the right-hand side in the upper line, the convolution by $\epsilon * \widetilde{\epsilon}$ on the second variable t_2 has been rewritten by moving ϵ out, while the rest is in fact $\overline{\langle yy\rangle}$ in Eq. (34)*. In the second term, the convolution by the Dirac on t_2 and we obtain two terms involving $\widetilde{\epsilon} * \lambda(t_1) = \langle y\rangle(t_1)$, see the solution for the 1st-order moment in Eq.* (32)*. Together, these three terms are the right-hand side of Eq.* (33)*, which is thus satisfied.*
Note also that $\widetilde{\epsilon}(t) = 0$ for $t < 0$ (reflecting causality of the overall "feedback' kernel), which implies that the operator $\widetilde{\epsilon} \overset{1}{*} \widetilde{\epsilon}\overset{2}{*}$ applied on the 2-dimensional function under the overline only "spreads" the function mass towards future (see Fig. 3B).
Case $p = 3$:
Following the previous section, we extend the calculations to the case $p = 3$ in order to prepare for the generalization to arbitrary $p \geq 2$. As with $p = 2$, we consider the ordering $t_1 \leq t_2 \leq t_3$ (purple subspace in Fig. 3C), which allows the development of the third time variable as was done in Eq. (33)

$$\overline{\langle yyy\rangle}(t_1, t_2, t_3) = \epsilon \overset{3}{*} \overline{\langle yyy\rangle}(t_1, t_2, t_3) + \overline{\langle yy\rangle\lambda}(t_1, t_2, t_3) + \overline{\langle yy\rangle\delta^{32}}(t_1, t_2, t_3) \ , \tag{36}$$

with the Dirac corresponding to the "boundary condition" when $t_3 \to t_2$, corresponding to the "lower" tilted plane of the purple subspace to which points the blue arrow in Fig. 3B. Note that this involves only the atomic contribution δ^{32} (δ^{21} is in yy corresponding to (t_1, t_2)), the other δ^{31} alone is not possible in this space. See also the discussion in Example 1 for the second-order input moments. Now we pursue the calculations without the time variables in arguments, as before for $p = 2$. The putative symmetric solution is

$$\overline{\langle yyy\rangle} = \widetilde{\epsilon} \overset{1}{*} \widetilde{\epsilon} \overset{2}{*} \widetilde{\epsilon} \overset{3}{*} (\overline{\lambda\lambda\lambda} + \overline{\lambda\lambda\delta^{32}} + \overline{\lambda\lambda\delta^{31}} + \overline{\lambda\delta^{21}\lambda} + \overline{\lambda\delta^{21}\delta^{32}}) \ , \tag{37}$$

which involves the contractions for all partitions of $\{1, 2, 3\}$, in a similar fashion to Eq. (21)*. We use again Eq.* (30) *as in Eq.* (35) *to obtain the convolution of ϵ with $\overline{\langle yyy\rangle}$ on t_3 and regroup the other terms where the convolution with t_3 vanishes because of the Dirac in order to use the expression of the 2nd-order moment in Eq.* (34)*, namely $\widetilde{\epsilon} \overset{1}{*} \widetilde{\epsilon} \overset{2}{*} (\overline{\lambda\lambda} + \overline{\lambda\delta^{21}}) = \overline{\langle yy\rangle}$:*

$$\begin{aligned} \overline{\langle yyy\rangle} &= \epsilon \overset{3}{*} \overline{\langle yyy\rangle} + \widetilde{\epsilon} \overset{1}{*} \widetilde{\epsilon} \overset{2}{*} (\overline{\lambda\lambda\lambda} + \overline{\lambda\delta^{21}\lambda}) + \widetilde{\epsilon} \overset{1}{*} \widetilde{\epsilon} \overset{2}{*} (\overline{\lambda\lambda\delta^{32}} + \overline{\lambda\delta^{21}\delta^{32}}) + \widetilde{\epsilon} \overset{1}{*} \widetilde{\epsilon} \overset{2}{*} \overline{\lambda\lambda\delta^{31}} \\ &= \epsilon \overset{3}{*} \overline{\langle yyy\rangle} + \overline{\langle yy\rangle\lambda} + \overline{\langle yy\rangle\delta^{32}} + \widetilde{\epsilon} \overset{1}{*} \widetilde{\epsilon} \overset{2}{*} \overline{\lambda\lambda\delta^{31}} \ . \end{aligned} \tag{38}$$

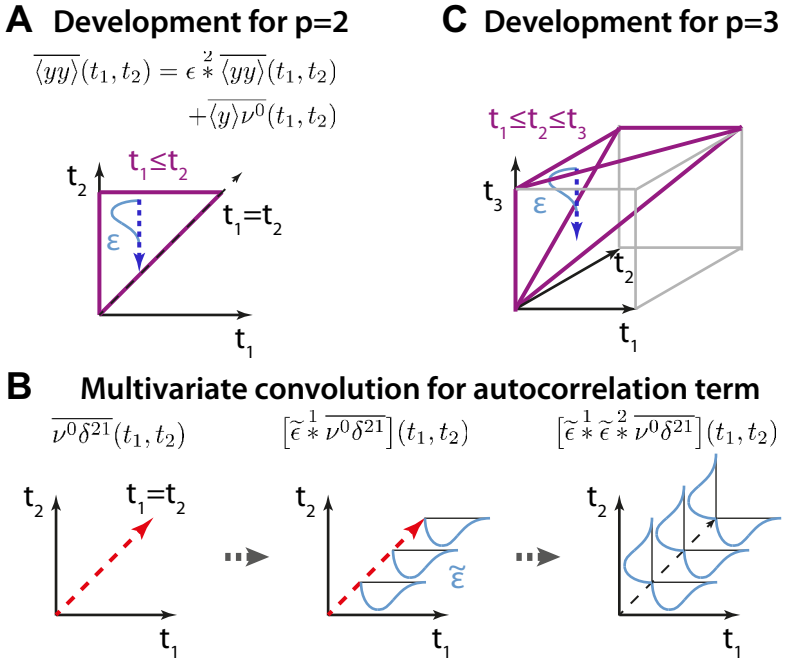

Figure 3: **Schematic diagrams supporting the calculations for the 2nd- and 3rd-order moments. A:** The development in Eq. (33) corresponds in expressing $y(t_2)$ as a function of the past history. This requires that $t_2 > t_1$, as illustrated by the purple upper triangle of the plane. The blue arrow indicates the "direction" of the development towards the past network activity, which is necessary to evaluate the firing probabilities involved in the moment. **B:** Schematic representation of the twofold convolution involved in Eq. (34) for the calculation of the second-order moment. The Dirac delta correspond to a function that is non-zero on the diagonal $t_1 = t_2$ only. The effect of the first convolution on t_1 "spreads" the diagonal function towards the "future" in the horizontal direction. Then, the convolution on t_2 "spreads" the whole towards the "future" in the vertical direction, resulting in a symmetric function. Note that the result is distinct from outer product of the time vectors $\overline{(\widetilde{\epsilon} * \lambda)(\widetilde{\epsilon} * \lambda)}$. **C:** Similar diagram as panel A to indicate the subspace for the condition $t_1 \leq t_2 \leq t_3$ and represent the development of the moment for $p = 3$ in Eq. (36).

What remains to be seen is that the condition $t_1 \leq t_2 \leq t_3$ implies that $\delta^{31} = 0$ always: when $t_1 = t_3$, in fact we have $t_1 = t_2 = t_3$, which corresponds to $\delta^{21}\delta^{31}$. This means that the last term in Eq. (38) *vanishes and Eq.* (36) *is satisfied. The symmetry argument ensures the validity over all (t_1, t_2, t_3), as will be formalized below.*

Numerical simulation:

The upper plot in Fig. 4A illustrates that the rhythm of the output spiking is altered by the recurrent self-connection. This comes from the fact that, for an excitatory self-connection, output spikes momentarily increase the firing rate, as can be seen when comparing the green curve with the dotted black curve in the bottom plot. The output first-order moment in Fig. 4B (solid gray curve for the simulation and dashed black curve for the prediction) is above the input first-order moment related to the underlying firing rate λ (dotted black curve). Note also the shift to later time.

The decomposition of the second-order moment in Fig. 4C illustrates that the effect of autocorrelations (right plot) spreads from the diagonal due to the self-connection. The main diagonal for $p = 2$ in Fig. 4D has larger values than the curve for $p = 1$ in Fig. 4B. In Fig. 4E, the main diagonal for $p = 3$ (cyan curve) is even larger, indicating that effects due to autocorrelation cumulate (as for input moments in Fig. 2).

The slices of the output third-order moment in Fig. 4E has different scales, but note the high spike density along the diagonal of the red matrix, due to the spreading of atomic contributions by the recurrent kernel ϵ.

Theorem 2 (Input-output mapping for recurrent connectivity) *The moment $Y_{\mathbf{i}}^p$ of order p of the Hawkes process (definition 1) of the network population can be expressed as*

$$Y_{\mathbf{i}}^p(\mathbf{t}) = \left(\widetilde{\boldsymbol{\epsilon}}_{\mathbf{ij}}^p \circledast Y_{\mathbf{j}}^{p,\epsilon=0}\right)(\mathbf{t}) \ . \tag{39}$$

The effects of the recurrent connectivity on the input moments are determined by spatio-temporal filtering described by the effective recurrent kernel $\widetilde{\boldsymbol{\epsilon}}^p$ defined similarly to Eq. (17) *on the moment for uncoupled neurons in Eq.* (21)*.*

Proof of Theorem 2: Compared to Example 2, we consider the general case where inputs and/or spontaneous activity drive the network neurons via $\nu^{\epsilon=0}$ in Eq. (15). Let introduce the *conditional moment* $M_{\mathbf{i}}^p(\mathbf{t})$ of order p defined as

$$M_{\mathbf{i}}^p(\mathbf{t}) \equiv \left\langle \prod_{r=1}^{p} y_{i_r}(t_r) \right\rangle_{y|x,\lambda} , \tag{40}$$

where the conditioning is over the input activity x and the spontaneous activity λ. Note that the statistical averaging over x and λ of the conditional moment gives the (unconditional) moment defined in Eq. (7): $\left\langle M_{\mathbf{i}}^p(\mathbf{t}) \right\rangle_{x,\lambda} = Y_{\mathbf{i}}^p(\mathbf{t})$. To demonstrate Eq. (39), we prove by induction the following result on $M_{\mathbf{i}}^p(\mathbf{t})$, which straightforwardly leads to the expression in Theorem 2 by taking the same statistical averaging over x and λ as done above:

$$M_{\mathbf{i}}^p(\mathbf{t}) = \left(\widetilde{\boldsymbol{\epsilon}}_{\mathbf{ij}}^p \circledast M_{\mathbf{j}}^{p,\epsilon=0}\right)(\mathbf{t}) \ , \tag{41}$$

where the conditional moment of order p in the absence of recurrent coupling ($\epsilon = 0$) is defined as

$$M_{\mathbf{j}}^{p,\epsilon=0}(\mathbf{t}) = \sum_{\Phi \in \mathcal{P}_p} \prod_{S \in \Phi} \delta_{\mathbf{j}_S}(\mathbf{t}_S) \ \nu_{j_{\check{S}}}^{\epsilon=0}(t_{\check{S}}) \tag{42}$$

In Eq. (41) the effect of the past spiking activity of y due to the recurrent connectivity ϵ is taken care of by all $\widetilde{\epsilon}$, considering $\nu^{\epsilon=0}$ to be "deterministic" from the viewpoint of y provided x and λ are known.

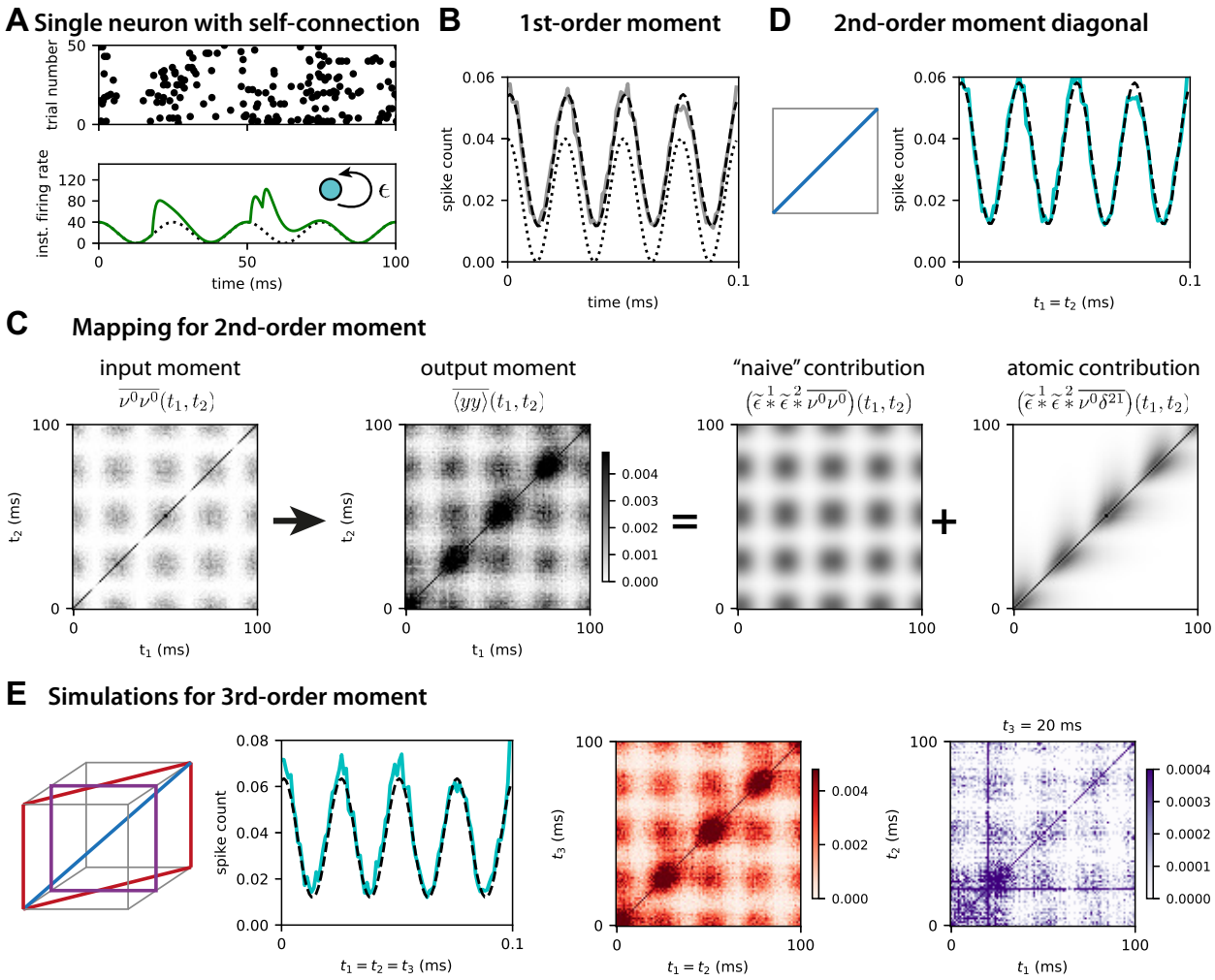

Figure 4: **Output moments for a single neuron with self-connection. A:** Spike raster (top plot) for 50 simulations for a neuron, similar to Fig. 2. In the bottom plot, the oscillatory rate function λ (dotted black curve) is compared with the instantaneous firing rate ν (green curve), which is affected by the neuron's firing. **B:** 1st-order moment (solid gray curve) with theoretical prediction (dashed black curve). The dotted black curve indicate the underlying firing rate λ. **C:** The two left plots represent the Input-output mapping for the 2nd-order moment, averaged over 10000 simulations (darker pixels indicate a higher spike density). The two right plots illustrate the decomposition into a contribution due to rate correlation (co-fluctuations, "naive" contribution) and that due to autocorrelation. Note that the right plot corresponds to Fig. 3B. The equations above refer to the terms in Eq. (35). **D:** Simulation (cyan curve) and theoretical prediction (dashed black curve) of the diagonal of the matrix for the output moment in panel C. **E:** Example slices for the 3rd-order moment, as indicated by the left diagram (color coded). All prediction curves are calculated using Eqs. (35) and (38).

The *conditioned moment* $M^p_{\mathbf{i}}(\mathbf{t})$ in Eq. (41) must obey the constraints imposed by the dynamics in Eq. (1). Under the condition on the time variables $t_1 \leq \cdots \leq t_p$, we can develop for $y_{i_p}(t_p)$ using the past activity of $(y_1(t), \cdots, y_p(t))$ for $t < t_p$ and the driving rate function $\nu^{\epsilon=0}_{i_p}(t_p)$. Let $\mathbf{i} = (i_1, \cdots, i_p)$ denote the coordinates and $\mathbf{t} = (t_1, \cdots, t_p)$ the time variables. The p^{th} order correlation of the output population can be expressed as

$$\begin{aligned} M^p_{\mathbf{i}}(\mathbf{t}) &= \left\langle \prod_{r=1}^{p} y_{i_r}(t_r) \right\rangle_{y|x,\lambda} \\ &= \left\langle \prod_{r=1}^{p-1} y_{i_r}(t_r) \cdot \nu_{i_p}(t_p) \right\rangle_{y|x,\lambda} + \left\langle \prod_{r=1}^{p-1} y_{i_r}(t_r) \right\rangle_{y|x,\lambda} \delta_{i_{p-1} i_p}(t_{p-1}, t_p) \ . \end{aligned} \tag{43}$$

Note that the generalized delta corresponds to the "boundary condition" $t_p = t_{p-1}$, as done in the above examples to moments. A similar condition for the time lag was used in the case of covariances (Hawkes 1971a; Gilson, Burkitt, Grayden, Thomas, and van Hemmen 2009b). By using the development of $\nu_i(t) = (\epsilon_{ij} * y_j)(t) + \nu^{\epsilon=0}_i(t)$, see Eqs. (1) and (15) and by setting $\mathbf{i}' = (i_1, \cdots, i_{p-1})$ which contains the $p-1$ first elements of $\mathbf{i}$, and similarly $\mathbf{t}' = (t_1, \cdots, t_{p-1})$, we have

$$\begin{aligned} M^p_{\mathbf{i}}(\mathbf{t}) &= \left(\epsilon_{i_p,j_p} \overset{p}{*} M^p_{\mathbf{i}' j_p}\right)(\mathbf{t}) + \left\langle \prod_{r=1}^{p-1} y_{i_r}(t_r) \cdot \nu^{\epsilon=0}_{i_p}(t_p) \right\rangle_{y|x,\lambda} + \left\langle \prod_{r=1}^{p-1} y_{i_r}(t_r) \right\rangle_{y|x,\lambda} \delta_{i_{p-1} i_p}(t_{p-1}, t_p) \\ &= \left(\epsilon_{i_p,j_p} \overset{p}{*} M^p_{\mathbf{i}' j_p}\right)(\mathbf{t}) + M^{p-1}_{\mathbf{i}'}(\mathbf{t}') \ \left[\nu^{\epsilon=0}_{i_p}(t_p) + \delta_{i_{p-1} i_p}(t_{p-1}, t_p)\right] \ . \end{aligned} \tag{44}$$

where the conditioned moment of order $p-1$ appears in the right-hand side. Therefore, we can use Eq. (41) for the order $p-1$:

$$\begin{aligned} & M^{p-1}_{\mathbf{i}'}(\mathbf{t}') \ \left[\nu^{\epsilon=0}_{i_p}(t_p) + \delta_{i_{p-1} i_p}(t_{p-1}, t_p)\right] \\ &= \left(\widetilde{\boldsymbol{\epsilon}}^{p-1}_{\mathbf{i}'\mathbf{j}'} \circledast M^{p-1,\epsilon=0}_{\mathbf{j}'}\right)(\mathbf{t}') \ \left[\nu^{\epsilon=0}_{i_p}(t_p) + \delta_{i_{p-1} i_p}(t_{p-1}, t_p)\right] \\ &= \widetilde{\boldsymbol{\epsilon}}^{p-1}_{\mathbf{i}'\mathbf{j}'} \overset{p-1}{\circledast} \left[\sum_{\Phi \in \mathcal{P}^0_{p-1}} \prod_{S \in \Phi} \delta_{\mathbf{j}_S}(\mathbf{t}_S) \ \nu^{\epsilon=0}_{j_{\check{S}}}(t_{\check{S}}) \left[\nu^{\epsilon=0}_{i_p}(t_p) + \delta_{i_{p-1} i_p}(t_{p-1}, t_p)\right]\right] \\ &= \widetilde{\boldsymbol{\epsilon}}^{p-1}_{\mathbf{i}'\mathbf{j}'} \overset{p-1}{\circledast} \left(\sum_{\Phi \in \mathcal{P}^0_p} \prod_{S \in \Phi} \delta_{\mathbf{j}_S}(\mathbf{t}_S) \ \nu^{\epsilon=0}_{j_{\check{S}}}(t_{\check{S}})\right) \\ &= \widetilde{\boldsymbol{\epsilon}}^{p-1}_{\mathbf{i}'\mathbf{j}'} \overset{p-1}{\circledast} M^{p,\epsilon=0}_{\mathbf{j}' i_p}(\mathbf{t}) \ . \end{aligned} \tag{45}$$

Note that the tensor convolution $\overset{p-1}{\circledast}$ applies to the first $p-1$ indices $j' = (j_1, \cdots, j_{p-1})$ of the tensor of dimension p. In the third line of Eq. (45), we only retain the partitions that contribute to the summation under the condition $t_1 \leq \cdots \leq t_p$. To do so we define the subset $\mathcal{P}^0_{p-1} \subset \mathcal{P}_{p-1}$ of ordered partitions Φ, where the groups $S \in \Phi$ consist of all successive indices between $\check{S} = \min(S)$ and $\max(S)$ (equal for singletons). Following, we integrate the elements in the squared brackets to the sum by augmenting the partitions $\Phi \in \mathcal{P}^0_{p-1}$ to partitions in $\mathcal{P}^0_p$. Note that the passage from the second line to the fifth line in Eq. (45) also corresponds to taking $\epsilon = 0$ in Eq. (43).
Going back to Eq. (44), we isolate $M^p_{\mathbf{i}}(\mathbf{t})$ on the left-hand side:

$$\left(\kappa_{i_p,j_p} \overset{p}{*} M^p_{\mathbf{i}' j_p}\right)(\mathbf{t}) = \widetilde{\boldsymbol{\epsilon}}^{p-1}_{\mathbf{i}'\mathbf{j}'} \overset{p-1}{\circledast} M^{p,\epsilon=0}_{\mathbf{j}' i_p}(\mathbf{t}) \ , \tag{46}$$

where $\kappa_{ij}(t) \equiv \delta_{ij}(t,0) - \epsilon_{ij}(t)$ (see Prop 1). Using the property of $\widetilde{\epsilon}$ in Eq. (30), we obtain

$$\begin{aligned} M^p_{\mathbf{i}}(\mathbf{t}) &= \left[\widetilde{\epsilon}_{i_p j'_p} \overset{p}{*} \left(\kappa_{j'_p,j_p} \overset{p}{*} M^p_{\mathbf{i}' j_p}\right)\right](\mathbf{t}) \\ &= \left(\widetilde{\epsilon}_{i_p j_p} \overset{p}{*} \left(\widetilde{\boldsymbol{\epsilon}}^{p-1}_{\mathbf{i}'\mathbf{j}'} \overset{p-1}{\circledast} M^{p,\epsilon=0}_{\mathbf{j}' j_p}\right)\right)(\mathbf{t}) \\ &= \left(\widetilde{\boldsymbol{\epsilon}}^p_{\mathbf{ij}} \circledast M^{p,\epsilon=0}_{\mathbf{j}}\right)(\mathbf{t}) \ . \end{aligned} \tag{47}$$

Note so far we have only established the validity of this result for $t_1 \leq \cdots \leq t_p$. As said above, this is equivalent of considering only ordered partitions $\mathcal{P}^0_p$. The generalization to an arbitrary $\mathbf{t} = (t_1, \cdots, t_p)$ can be obtained by noting that an arbitrary $\mathbf{t} = (t_1, \cdots, t_p)$ can be mapped to an ordered version using permutations, say $\Pi(\mathbf{t}) = \mathbf{t}' = (t'_1 \leq \cdots \leq t'_p)$. The partition set $\mathcal{P}^0_p$ is thus replaced by $\left\{\Pi(\Phi), \Phi \in \mathcal{P}^0_p\right\}$ with $\Pi(\Phi)$ being the partition of the image indices via Π. Note that this covers entire set of all partitions $\mathcal{P}_p$ when considering all possible permutations. This concludes the proof by induction.

□

Remark 5 (Large population size) *In the limit of large population size ($n \to \infty$) and in the absence of the driving rates ($\lambda = 0$), the output moment of order p can simply be approximated by the single dominating term*

$$Y^p_{\mathbf{i}}(\mathbf{t}) \simeq \left(\widetilde{\boldsymbol{\epsilon}}^p_{\mathbf{ij}} \circledast \boldsymbol{\gamma}^p_{\mathbf{jk}} \circledast X^p_{\mathbf{k}}\right)(\mathbf{t}) \tag{48}$$

This corresponds to the partition $\Phi = \{I_p\}$ and has a contribution of order n^p whereas all other partitions $\Phi' \neq \Phi$ give a contribution of order $n^{p-|\Phi'|+1} \ll n^p$ which is negligible.

3 Relationship with cumulants

We end with relating our results with previous work (Jovanović, Hertz, and Rotter 2015; Ocker, Josić, Shea-Brown, and Buice 2017) focused on cumulants instead of moments, which is an alternative manner to describe the spiking statistics in the network. The genuine relationship between moments and cumulants appears via their generating functions (Daley and Vere-Jones 1988; Balakrishnan, Johnson, and Kotz 1998). Let $E(\boldsymbol{\zeta}, \mathbf{k}, \mathbf{t})$ be the moment generating function for the multivariate input $x_{\mathbf{k}}(\mathbf{t}) = (x_{k_1}(t_1), \cdots, x_{k_p}(t_p))$:

$$E(\boldsymbol{\zeta}, \mathbf{k}, \mathbf{t}) = \left\langle \exp\left(\sum_{r=1}^{p} \zeta_r x_{k_r}(t_r)\right)\right\rangle_x \ , \tag{49}$$

where $\boldsymbol{\zeta} = (\zeta_1, \cdots, \zeta_p)^T$. This moment generating function can be used to express the p^{th} order moment over the coordinates $\mathbf{k}$ and times $\mathbf{t}$:

$$X^p_{\mathbf{k}}(\mathbf{t}) = \frac{\partial^p E(\boldsymbol{\zeta}, \mathbf{k}, \mathbf{t})}{\partial \zeta_{i_1} \cdots \partial \zeta_p}\Big|_{\boldsymbol{\zeta}=0} \equiv \frac{\partial^p E(\boldsymbol{\zeta}, \mathbf{k}, \mathbf{t})}{\partial \boldsymbol{\zeta}}\Big|_{\boldsymbol{\zeta}=0} \tag{50}$$

Similarly, the cumulant generating function

$$K(\boldsymbol{\zeta}, \mathbf{k}, \mathbf{t}) \equiv \log E(\boldsymbol{\zeta}, \mathbf{k}, \mathbf{t}) \tag{51}$$

allows for the calculation of the input cumulants $\bar{X}^p_{\mathbf{k}}(\mathbf{t})$ of order p:

$$\bar{X}^p_{\mathbf{k}}(\mathbf{t}) = \frac{\partial^p K(\boldsymbol{\zeta}, \mathbf{k}, \mathbf{t})}{\partial \boldsymbol{\zeta}}\Big|_{\boldsymbol{\zeta}=0} \tag{52}$$

Property 2 *The formal relationship between the moment* $X^p_{\mathbf{k}}(\mathbf{t})$ *of order* p *and cumulants* $\bar{X}^{p'}_{\mathbf{k}'}(\mathbf{t}')$ *of order* $p' \leq p$ *—here presented for the inputs— is given by*

$$X^p_{\mathbf{k}}(\mathbf{t}) = \sum_{\Phi \in \mathcal{P}_p} \prod_{S \in \Phi} \bar{X}^{|S|}_{\mathbf{k}_S}(\mathbf{t}_S) \ , \tag{53}$$

where Φ *are the partitions of* I_p *composed of disjoint subsets* S*.*

Proof of Property 2: The present proof —inspired by previous work (Daley and Vere-Jones 1988; Balakrishnan, Johnson, and Kotz 1998)— relies on the following general result for the (partial) derivative of $\exp(f)$ with respect to variables $\boldsymbol{\zeta} = (\zeta_1, \cdots, \zeta_p)$ for an arbitrary function f without specified arguments:

$$\frac{\partial^p \exp(f)}{\partial \boldsymbol{\zeta}} \equiv \frac{\partial^p \exp(f)}{\partial \zeta_1 \cdots \partial \zeta_p} = \left(\sum_{\Phi \in \mathcal{P}_p} \prod_{S \in \Phi} \frac{\partial^{|S|} f}{\partial \boldsymbol{\zeta}_S} \right) \exp(f) \ , \tag{54}$$

which involves all partitions $\Phi \in \mathcal{P}_p$ and the partial derivatives $\frac{\partial^{|S|} f}{\partial \boldsymbol{\zeta}_S}$ of order $|S|$ with respect to the variables ζ_r whose indices $r \in S$. For $p = 1$ with ζ_1, we have the univariate case

$$\frac{\partial \exp(f)}{\partial \zeta_1} = \frac{\partial f}{\partial \zeta_1} \exp(f) \ . \tag{55}$$

To demonstrate Eq. (54), we assume the expression to be valid for $p-1$ and derive it for p, using a proof by induction. Separating ζ_p from the remaining variables $\boldsymbol{\zeta}' = (\zeta_1, \cdots, \zeta_{p-1})$, we use Eq. (54) for $p-1$:

$$\begin{aligned}
\frac{\partial^p \exp(f)}{\partial \boldsymbol{\zeta}} &= \frac{\partial}{\partial \zeta_p} \frac{\partial^{p-1} \exp(f)}{\partial \boldsymbol{\zeta}'} \\
&= \frac{\partial}{\partial \zeta_p} \left[\left(\sum_{\Phi \in \mathcal{P}_{p-1}} \prod_{S \in \Phi} \frac{\partial^{|S|} f}{\partial \boldsymbol{\zeta}_S} \right) \exp(f) \right] \\
&= \left[\sum_{\Phi \in \mathcal{P}_{p-1}} \frac{\partial}{\partial \zeta_p} \left(\prod_{S \in \Phi} \frac{\partial^{|S|} f}{\partial \boldsymbol{\zeta}_S} \right) \right] \exp(f) + \left(\sum_{\Phi \in \mathcal{P}_{p-1}} \prod_{S \in \Phi} \frac{\partial^{|S|} f}{\partial \boldsymbol{\zeta}_S} \right) \frac{\partial f}{\partial \zeta_p} \exp(f)
\end{aligned} \tag{56}$$

where the derivative with respect to ζ_p applied to the product yields two terms. The second term corresponds to Eq. (55), which can be assimilated to the partition $\Phi' \in \mathcal{P}_p$ such that $\Phi' = \Phi \cup \{ \{p\} \}$. The first term actually gives $|\Phi|$ terms, one for each subset S of the product, which depends on the actual partition Φ. For each Φ, we construct $|S|$ partitions $\Phi' \in \mathcal{P}_p$ by adding the index p to one of the subsets $S \in \Phi$. Because a partition $\Phi \in \mathcal{P}_p$ can only be of one of the two types, we end up with

$$\begin{aligned}
\frac{\partial^p \exp(f)}{\partial \boldsymbol{\zeta}} &= \left(\sum_{\Phi \in \mathcal{P}_p \setminus \mathcal{Q}_p} \prod_{S \in \Phi} \frac{\partial^{|S|} f}{\partial \boldsymbol{\zeta}_S} + \sum_{\Phi \in \mathcal{Q}_p} \prod_{S \in \Phi} \frac{\partial^{|S|} f}{\partial \boldsymbol{\zeta}_S} \right) \exp(f) \\
&= \left(\sum_{\Phi \in \mathcal{P}_p} \prod_{S \in \Phi} \frac{\partial^{|S|} f}{\partial \boldsymbol{\zeta}_S} \right) \exp(f) \ ,
\end{aligned} \tag{57}$$

where $\mathcal{Q}_p = \{\Phi \in \mathcal{P}_p, \{p\} \in \Phi\}$ is the set of all partitions of I_p that contain the singleton $\{p\}$.

Coming back to the moments, we prove Eq. (53) by applying Eq. (54) to the function $K(\zeta, \mathbf{k}, \mathbf{t})$:

$$\begin{aligned} X^p_{\mathbf{k}}(\mathbf{t}) &= \frac{\partial^p \exp\left[K(\boldsymbol{\zeta}, \mathbf{k}, \mathbf{t})\right]}{\partial \boldsymbol{\zeta}}\Big|_{\boldsymbol{\zeta}=0} \\ &= \sum_{\Phi \in \mathcal{P}_p} \prod_{S \in \Phi} \frac{\partial^{|S|} K(\boldsymbol{\zeta}, \mathbf{k}, \mathbf{t})}{\partial \boldsymbol{\zeta}_S} \exp\left(K\left(\boldsymbol{\zeta}, \mathbf{k}, \mathbf{t}\right)\right)\Big|_{\boldsymbol{\zeta}=0} \\ &= \sum_{\Phi \in \mathcal{P}_p} \prod_{S \in \Phi} \bar{X}^{|S|}_{\mathbf{k}_S}(\mathbf{t}_S) \ , \end{aligned} \tag{58}$$

after noticing that $\exp\left(K\left(\mathbf{0}, \mathbf{k}, \mathbf{t}\right)\right) = 1$. □

Corollary 1 *A direct corollary of Proposition 2 is that, when the input neurons are independent and of rate $\mu_k(t_k)$, then the cumulant of order p of the input population x is given by*

$$\bar{X}^p_{\mathbf{k}}(\mathbf{t}) = \delta_{\mathbf{k}}(\mathbf{t})\ \mu_{k_1}(t_1) \ . \tag{59}$$

The proof simply consists in identifying the terms in Eq. (12) to the cumulants, where $\mathbf{k}$ and $\mathbf{t}$ are respectively replaced by $\mathbf{k}_S$ and $\mathbf{t}_S$ for each subset S.

Now we examine the general situation of a network with afferent and recurrent connectivities, corresponding to the combined theorems for moments —see Eqs. (21) and (39). We define the cumulant of order p for the spontaneous rate, filtered inputs and and outputs —namely $\bar{\Lambda}_{\mathbf{i}}(\mathbf{t})$, $\bar{\Gamma}_{\mathbf{i}}(\mathbf{t})$ and $\bar{Y}_{\mathbf{i}}(\mathbf{t})$— in the same manner as in Eq. (52) for inputs.

Theorem 3 (Mappings for cumulants) *The cumulants are related by the following mappings:*

$$\bar{\Gamma}^p_{\mathbf{i}}(\mathbf{t}) = \left(\boldsymbol{\gamma}^p_{\mathbf{ik}} \circledast \bar{X}^p_{\mathbf{k}}\right)(\mathbf{t}) \ , \tag{60a}$$

$$\bar{Y}^{p,\epsilon=0}_{\mathbf{i}}(\mathbf{t}) = \sum_{\Phi \in \mathcal{P}_p} \left[\prod_{S \in \Phi} \delta_{\mathbf{i}_S}(\mathbf{t}_S)\right] \left[\bar{\Gamma}^{|\check{\Phi}|}_{\mathbf{i}_{\check{\Phi}}}(\mathbf{t}_{\check{\Phi}}) + \bar{\Lambda}^{|\check{\Phi}|}_{\mathbf{i}_{\check{\Phi}}}(\mathbf{t}_{\check{\Phi}})\right] \ , \tag{60b}$$

$$\bar{Y}^p_{\mathbf{i}}(\mathbf{t}) = \left(\widetilde{\boldsymbol{\epsilon}}^p_{\mathbf{ij}} \circledast \bar{Y}^{p,\epsilon=0}_{\mathbf{j}}\right)(\mathbf{t}) \ . \tag{60c}$$

Proof of Theorem 3: Eq. (60a) simply comes from the linearity of the filtering by γ. Another manner to prove it is to decompose the moment in terms of cumulants, as we do now to demonstrate Eq. (60c).

By rewriting Eq. (39) in terms of cumulants using Eq. (53), we have

$$\begin{aligned} \sum_{\Phi \in \mathcal{P}_p} \prod_{S \in \Phi} \bar{Y}^{|S|}_{\mathbf{i}_S}(\mathbf{t}_S) &= \widetilde{\boldsymbol{\epsilon}}_{\mathbf{ij}} \circledast \left(\sum_{\Phi \in \mathcal{P}_p} \prod_{S \in \Phi} \bar{Y}^{|S|,\epsilon=0}_{\mathbf{j}_S}(\mathbf{t}_S)\right) \\ &= \sum_{\Phi \in \mathcal{P}_p} \prod_{S \in \Phi} \left(\widetilde{\boldsymbol{\epsilon}}_{\mathbf{i}_S\mathbf{j}_S} \circledast \bar{Y}^{|S|,\epsilon=0}_{\mathbf{j}_S}\right)(\mathbf{t}_S) \ . \end{aligned} \tag{61}$$

As before, we identify the terms for each S and Φ.

In contrast, Eq. (60b) is not straightforward and comes from the spiking nature of y driven by a function $\nu^{\epsilon=0}$ that possibly has high-order correlations (for example a Cox process). Basically, it is the extension of cumulants of smaller orders by delta functions for all possible partitions for each time variable of the smaller-order cumulant. For simplicity, we only show the result

for $\bar{\Gamma}$; note also that the additivity of the cumulant ensures the complete result. We rewrite Eq. (26) —that is the equivalent of Eq. (21) in the absence of λ— in terms of cumulants using Eq. (53):

$$\sum_{\Phi\in\mathcal{P}_p}\prod_{S\in\Phi}\bar{Y}^{|S|,\epsilon=0}_{\mathbf{i}_S}(\mathbf{t}_S)=\sum_{\Phi\in\mathcal{P}_p}\left(\prod_{S\in\Phi}\check{\delta}_{\mathbf{i}_S}(\mathbf{t}_S)\right)\left[\sum_{\Phi'\in\mathcal{P}(\check{\Phi})}\prod_{S'\in\Phi'}\bar{\Gamma}^{|S'|}_{\mathbf{i}_{S'}}(\mathbf{t}_{S'})\right] . \tag{62}$$

In Eq. (62) cumulants $\bar{\Gamma}$ involve indices from distinct subsets S of the partition Φ, as they "combine" the minima in $\check{\Phi}$ according to Φ'. We now reorganize the expression to obtain a similar expression to the left-hand side, where the terms in the product over S have a generic expression with indices only in S. The product of generalized delta functions can be moved inside the sum over Φ', yielding

$$\sum_{\Phi\in\mathcal{P}_p}\prod_{S\in\Phi}\bar{Y}^{|S|,\epsilon=0}_{\mathbf{i}_S}(\mathbf{t}_S)=\sum_{\Phi\in\mathcal{P}_p}\sum_{\Phi'\in\mathcal{P}(\check{\Phi})}\left(\prod_{S\in\Phi}\check{\delta}_{\mathbf{i}_S}(\mathbf{t}_S)\right)\left(\prod_{S'\in\Phi'}\bar{\Gamma}^{|S'|}_{\mathbf{i}_{S'}}(\mathbf{t}_{S'})\right) . \tag{63}$$

For each pair of partitions Φ and Φ', we construct a partition $\Psi\in\mathcal{P}_p$, whose subsets T are the unions of subsets S corresponding to the same $S'\in\Phi'$:

$$T=\bigcup_{\substack{S\in\Phi,\\ \check{S}\in S'\in\Phi'}} S . \tag{64}$$

In addition, we define a partition $\Psi'_T\in\mathcal{P}(T)$ for each $T\in\Psi$ that splits T into the original subsets $S\in\Phi$:

$$\Psi'_T=\bigcup_{S\in T}\{S\} . \tag{65}$$

The correspondence between the partitions is represented in Fig. 5 for a schematic example. Using Eq. (65) with $S\equiv T'\in\Psi'_T$ for the each T, the first product in Eq. (63) can be rewritten as

$$\prod_{S\in\Phi}\check{\delta}_{\mathbf{i}_S}(\mathbf{t}_S)=\prod_{T\in\Psi}\prod_{T'\in\Psi'_T}\check{\delta}_{\mathbf{i}_{T'}}(\mathbf{t}_{T'}) . \tag{66}$$

Because each $S'\in\Phi'=\check{\Phi}$ is the subset of minima $\check{\Psi}'_T$ for the corresponding $T=\bigcup S$, we similarly reformulate the second product

$$\prod_{S'\in\Phi'}\bar{\Gamma}^{|S'|}_{\mathbf{i}_{S'}}(\mathbf{t}_{S'})=\prod_{T\in\Psi}\bar{\Gamma}^{|\check{\Psi}'_T|}_{\mathbf{i}_{\check{\Psi}'_T}}(\mathbf{t}_{\check{\Psi}'_T}) . \tag{67}$$

We can thus factorize the two products in the right-hand side of Eq. (63) to obtain

$$\left(\prod_{S\in\Phi}\check{\delta}_{\mathbf{i}_S}(\mathbf{t}_S)\right)\left(\prod_{S'\in\Phi'}\bar{\Gamma}^{|S'|}_{\mathbf{i}_{S'}}(\mathbf{t}_{S'})\right)=\prod_{T\in\Psi}\left(\prod_{T'\in\Psi'_T}\check{\delta}_{\mathbf{i}_{\check{T}'}}(\mathbf{t}_{\check{T}'})\right)\bar{\Gamma}^{|\check{\Psi}'_T|}_{\mathbf{i}_{\check{\Psi}'_T}}(\mathbf{t}_{\check{\Psi}'_T}) . \tag{68}$$

Last, the key observation is that each pair $\Phi\in\mathcal{P}_p$ and $\Phi'\in\mathcal{P}(\check{\Phi})$ is uniquely associated with another pair made of a partition $\Psi\in\mathcal{P}_p$ and its corresponding set of partitions $\{\Psi'_T\in\mathcal{P}(T)\}_{T\in\Psi}$:

$$(\Phi,\Phi')\leftrightarrow(\Psi,\{\Psi'_T\}_{T\in\Psi}) . \tag{69}$$

As a consequence, the double summation over Φ and Φ' in Eq. (63) can be expressed as a summation over Ψ and over its corresponding sub-partitions, namely

$$\sum_{\Phi\in\mathcal{P}_p}\sum_{\Phi'\in\mathcal{P}(\check{\Phi})}\leftrightarrow\sum_{\Psi\in\mathcal{P}_p}\sum_{\Psi'_{T_1}\in\mathcal{P}(T_1)}\cdots\sum_{\Psi'_{T_{|\Psi|}}\in\mathcal{P}(T_{|\Psi|})}\equiv\sum_{\Psi\in\mathcal{P}_p}\sum_{\substack{\Psi'_T\in\mathcal{P}(T),\\ \forall T\in\Psi}} , \tag{70}$$

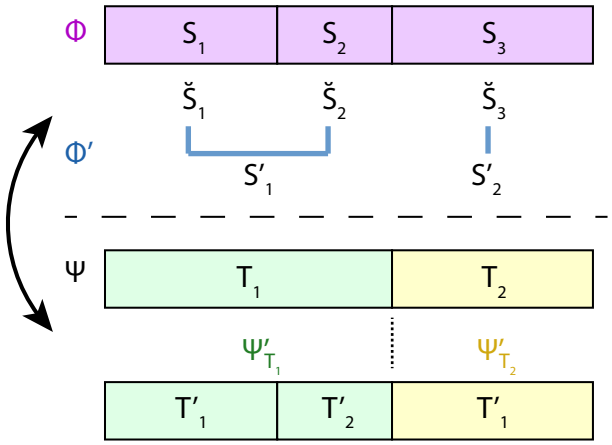

Figure 5: **One-to-one mapping between partitions.** The partition Ψ is constructed from the pair Φ and Φ'. To each element of $T \in \Psi$ corresponds a partition Ψ'_T that recovers the original subsets in Φ. See Eqs. (64) and (65) in the main text for the mathematical construction. Here the subsets are indexed as in Eq. (70) and the partitions are color-coded for legibility.

with the explicit enumeration of $T_r \in \Psi$. With this substitution, Eq. (63) can be expressed as:

$$\begin{aligned}\sum_{\Phi\in\mathcal{P}_p}\prod_{S\in\Phi}\bar{Y}^{|S|,\epsilon=0}_{\mathbf{i}_S}(\mathbf{t}_S) &= \sum_{\Psi\in\mathcal{P}_p}\sum_{\substack{\Psi'_T\in\mathcal{P}(T),\\ \forall T\in\Psi}}\prod_{T\in\Psi}\left(\prod_{T'\in\Psi'_T}\hat{\delta}_{\mathbf{i}_{T'}}(\mathbf{t}_{T'})\right)\bar{\Gamma}^{|\check{\Psi}'_T|}_{\mathbf{i}_{\check{\Psi}'_T}}(\mathbf{t}_{\check{\Psi}'_T}) \\ &= \sum_{\Psi\in\mathcal{P}_p}\prod_{T\in\Psi}\left[\sum_{\Psi'\in\mathcal{P}(T)}\left(\prod_{T'\in\Psi'}\hat{\delta}_{\mathbf{i}_{T'}}(\mathbf{t}_{T'})\right)\bar{\Gamma}^{|\check{\Psi}'|}_{\mathbf{i}_{\check{\Psi}'}}(\mathbf{t}_{\check{\Psi}'})\right] . \qquad (71)\end{aligned}$$

Once again, we conclude by identifying the terms for each T and Ψ in the right-hand side and S and Φ in the left-hand side of Eq. (71).

□

Note that Eq. (60b) for cumulants resembles its counterpart Eq. (21) for moments, but in the case where the neurons are stimulated by both inputs and a spontaneous firing rate, the corresponding cumulants are simply summed, whereas moments appear in a product.

4 Discussion

In this paper we analytically computed the statistics of neuronal activity in a recurrent network —described via moments and then transposed to cumulants— from the statistics of the input neuronal population. An important contribution of our study is the description of the propagation of spiking moments in feedforward networks (Theorem 1) and recurrently-connected networks (Theorem 2), which had not been explored before. Theorem 3 established the equivalent mappings for cumulants. Compared to recent studies for cumulants (Jovanović, Hertz, and Rotter 2015; Ocker, Josić, Shea-Brown, and Buice 2017), an important advantage of the operator viewpoint taken here is that it provides intuition about the spatio-temporal filtering induced by both afferent and recurrent connectivities.

The main technical challenge comes from the spiking nature of neurons which forces us to consider all possible contractions, see Eq. (3). For rate-based neurons —still interacting through spatio-temporal kernels— or equivalently assuming that the population size is very large such that individual spikes have negligible effects, our results can be expressed in a much simpler way (see Remark 5). In this case, the output moments can be approximated by a nested

convolution: a first convolution of the input moments with the feedforward kernel followed by a second convolution with the effective recurrent kernel. Quantifying the deviations from this approximation for neuronal population of finite size is left for future work.

At the heart of the tractability in this study is the linearity assumption of the Hawkes process, as the firing rate is linear in the membrane potential that simply sums the synaptic inputs. This obviously imposes limitations to the scope of the results presented here. For instance, inhibition, which is ubiquitous in the brain, cannot be exactly modeled with a purely mutually exciting process. A possibility to include a nonlinearity in the expression of the firing rate in terms of the synaptic inputs, but the mathematical literature that explored this direction is scarce (Brémaud and Massoulié 1996). Mean-field approximations lead to analytical results (Toyoizumi, Rad, and Paninski 2009), but they are only valid in the limit of weak coupling. Another possibility is to rely on path-integral formulation and the related Feynman diagram formalism (Ocker, Josić, Shea-Brown, and Buice 2017; Chen, Shojaie, Shea-Brown, and Witten 2018), but the complexity of the results might preclude an intuitive understanding of the combined effect of the feedforward and recurrent kernels in propagating spiking moments. Moreover, in the case of correlated inputs, the linear Hawkes process already leads to complex cross-overs between cumulants —as can be seen in Eq. (60b), which also relates to Cox processes (Lechnerová, Helisová, and Beneš 2008; Laier, Prokesova, and Jensen 2008)— and many more are expected to appear for the nonlinear case.

In the context of neuroscience, our results can be directly applied to the field of synaptic plasticity. For activity-dependent models, the expected weight change can be expressed from the corresponding statistics of the spiking activity (Kempter, Gerstner, and Van Hemmen 1999; Gilson, Burkitt, and van Hemmen 2010). Furthermore, since synaptic plasticity has been demonstrated to depend on higher-order correlations (Pfister and Gerstner 2006; Clopath, Büsing, Vasilaki, and Gerstner 2010), our formalism provides the adequate tools to analytically study synaptic plasticity in recurrently-connected networks, extending previous work that relied on approximations (Gjorgjieva, Clopath, Audet, and Pfister 2011).

Efforts have been made to fit univariate Hawkes processes to empirical time series using Bayesian estimation based on the likelihood (Ozaki 1979; Truccolo 2016; Laub, Taimre, and Pollett 2015; Fujita, Medvedev, Koyama, Lambiotte, and Shinomoto 2018) or relying on second-order statistics (Da Fonseca and Zaatour 2014; Bacry and Muzy 2016). Refinements have also been explored in the case of sparse observations of the network activity over time (Le 2018). It remains to be explored whether high-order moments can be useful for parameter estimation.

Last, as mentioned in Fig. 1, the difference between space and time here is simply their discrete and continuous natures. The moments tensors could also be defined with continuous space-time variables, adapting Eq. (18) with a spatial integral in line with previous work (Møller and Torrisi 2007). Because our proof relies on linear algebra, it can easily be extended to this new context.

Acknowledgments

MG acknowledges funding from European Union's Horizon 2020 research and innovation programme via the Marie Skłodowska-Curie Action (H2020-MSCA-656547) and under Grant Agreement No. 785907 (HBP SGA2). JPP was supported by the Swiss National Science Foundation (SNSF) grants PP00P3_150637 and PP00P3_179060.

References

Bacry, E., I. Mastromatteo, and J.-F. Muzy (2015). Hawkes processes in finance. *Mark Microstructure Liq 01*, 1550005.

Bacry, E. and J.-M. Muzy (2016). First- and second-order statistics characterization of hawkes processes and non-parametric estimation. *IEEE Information Theory Society 62*, 2184–2202.

Balakrishnan, N., N. L. Johnson, and S. Kotz (1998). A note on relationships between moments, central moments and cumulants from multivariate distributions. *Statistics & Probability Letters 39*, 49–54.

Barreiro, A. K., J. Gjorgjieva, F. Rieke, and E. Shea-Brown (2014). When do microcircuits produce beyond-pairwise correlations? *Front Comput Neurosci 8*, 10.

Brémaud, P. and L. Massoulié (1996). Stability of nonlinear hawkes processes. *Ann. Probab. 24*, 1563–1588.

Brémaud, P., L. Massoulié, and A. Ridolfi (2005). Power spectra of random spike fields and related processes. *Adv Appl Probab 4*, 1116–1146.

Chen, S., A. Shojaie, E. Shea-Brown, and D. Witten (2018). The multivariate hawkes process in high dimensions: Beyond mutual excitation. *arxiv*, 1707.04928.

Clopath, C., L. Büsing, E. Vasilaki, and W. Gerstner (2010, March). Connectivity reflects coding: a model of voltage-based STDP with homeostasis. *Nature Neuroscience 13*(3), 344–352.

Da Fonseca, J. and R. Zaatour (2014). Hawkes process: Fast calibration, application to trade clustering, and diffusive limit. *Journal of Futures Markets 34*, 548–579.

Dahmen, D., H. Bos, and M. Helias (2016). Correlated fluctuations in strongly coupled binary networks beyond equilibrium. *Phys. Rev. X 6*, 031024.

Daley, D. and D. Vere-Jones (1988). *An Introduction to the Theory of Point Processes.* Number 978-1-4757-2003-7. Springer.

Errais, E., K. Giesecke, and L. R. Goldberg (2010). Affine point processes and portfolio credit risk. *SIAM Journal on Financial Mathematics 1*, 642–665.

Etesami, J., N. Kiyavash, K. Zhang, and K. Singhal (2016). Learning network of multivariate hawkes processes: A time series approach. In *Proceedings of the Thirty-Second Conference on Uncertainty in Artificial Intelligence*, UAI'16, Arlington, Virginia, United States, pp. 162–171. AUAI Press.

Fujita, K., A. Medvedev, S. Koyama, R. Lambiotte, and S. Shinomoto (2018). Identifying exogenous and endogenous activity in social media. *arxiv*, 1808.00810.

Gilson, M., A. Burkitt, and L. J. van Hemmen (2010). Stdp in recurrent neuronal networks. *Front Comput Neurosci 4*, 23.

Gilson, M., A. N. Burkitt, D. B. Grayden, D. A. Thomas, and J. L. van Hemmen (2009a). Emergence of network structure due to spike-timing-dependent plasticity in recurrent neuronal networks I: Input selectivity–strengthening correlated input pathways. *Biol Cybern 101*, 81–102.

Gilson, M., A. N. Burkitt, D. B. Grayden, D. A. Thomas, and J. L. van Hemmen (2009b, Dec). Emergence of network structure due to spike-timing-dependent plasticity in recurrent neuronal networks IV: Structuring synaptic pathways among recurrent connections. *Biol Cybern 101*(5-6), 427–44.

Gjorgjieva, J., C. Clopath, J. Audet, and J.-P. Pfister (2011). A triplet spike-timing-dependent plasticity model generalizes the bienenstock–cooper–munro rule to higher-order spatiotemporal correlations. *Proceedings of the National Academy of Sciences 108*(48), 19383–19388.

Grytskyy, D., T. Tetzlaff, M. Diesmann, and M. Helias (2013). A unified view on weakly correlated recurrent networks. *Front Comput Neurosci 7*, 131.

Hawkes, A. (1971a). Point spectra of some mutually exciting point processes. *J Roy Stat Soc B 33*, 438–443.

Hawkes, A. (1971b). Spectra of some self-exciting and mutually exciting point processes. *Biometrika 58*, 83–90.

Helias, M., T. Tetzlaff, and M. Diesmann (2013). Echoes in correlated neural systems. *New journal of physics 15*, 023002.

Jovanović, S., J. Hertz, and S. Rotter (2015). Cumulants of hawkes point processes. *Phys Rev E 91*, 042802.

Kempter, R., W. Gerstner, and J. Van Hemmen (1999). Hebbian learning and spiking neurons. *Physical Review E 59*(4), 4498–4514.

Laier, G., M. Prokesova, and E. Jensen (2008). Lévy-based cox point processes. *Advances in Applied Probability 40*, 603–629.

Laub, P. J., T. Taimre, and P. K. Pollett (2015). Hawkes processes. *arxiv*, 1507.02822v1.

Le, T. M. (2018). A multivariate hawkes process with gaps in observations. *IEEE Transactions on Information Theory 64*(3), 1800–1811.

Lechnerová, R., K. Helisová, and V. Beneš (2008). Cox point processes driven by ornstein-uhlenbeck type processes. *Methodology and Computing in Applied Probability 10*, 315–335.

Lima, R. and J. Choi (2018). Make hawkes processes explainable by decomposing self-triggering kernels. *arxiv*, 1703.09068.

Mei, H. and J. M. Eisner (2017). The neural hawkes process: A neurally self-modulating multivariate point process. In I. Guyon, U. V. Luxburg, S. Bengio, H. Wallach, R. Fergus, S. Vishwanathan, and R. Garnett (Eds.), *Advances in Neural Information Processing Systems 30*, pp. 6754–6764. Curran Associates, Inc.

Møller, J. and G. L. Torrisi (2007). The pair correlation function of spatial hawkes processes. *Statistics and Probability Letters 77*(10), 995–1003.

Ocker, G., K. Josić, E. Shea-Brown, and M. Buice (2017). Linking structure and activity in nonlinear spiking networks. *PLoS Comput Biol 13*, e1005583.

Ozaki, T. (1979). Maximum likelihood estimation of hawkes' self-exciting point processes. *Ann Inst Stat Math 31*, 145.

Pfister, J.-P. and W. Gerstner (2006). Triplets of spikes in a model of spike timing-dependent plasticity. *J Neurosci 26*, 9673–9682.

Pfister, J.-P. and P. Tass (2010). STDP in oscillatory recurrent networks: theoretical condition for desynchronization and applications to deep brain stimulation. *Front Comput Neurosci 4*, 22.

Saichev, A., T. Maillart, and D. Sornette (2013). Hierarchy of temporal responses of multivariate self-excited epidemic processes. *Eur. Phys. J. B 86*, 124.

Shimazaki, H., K. Sadeghi, T. Ishikawa, Y. Ikegaya, and T. Toyoizumi (2015). Simultaneous silence organizes structured higher-order interactions in neural populations. *Sci Rep 5*, 9821.

Tannenbaum, N. R. and Y. Burak (2017). Theory of nonstationary hawkes processes. *Phys Rev E 96*, 062314.

Toyoizumi, T., K. Rad, and L. Paninski (2009). Mean-field approximations for coupled populations of generalized linear model spiking neurons with Markov refractoriness. *Neural Computation 21*(5), 1203–1243.

Truccolo, W. (2016). From point process observations to collective neural dynamics: Nonlinear hawkes process glms, low-dimensional dynamics and coarse graining. *Journal of Physiology Paris 110*, 336–347.

van Albada, S. J., M. Helias, and M. Diesmann (2015). Scalability of asynchronous networks is limited by one-to-one mapping between effective connectivity and correlations. *PLoS Comput Biol 11*, e1004490.